

https://dspace.org/

A mathematical model of a diaphragm-type chlor-alkali cell

Cook, Peter Gavin

2015-01-15
http://hdl.handle.net/10539/16536

Downloaded from a DSpace repository. https://dspace.org/

A MATHEMATICAL MODEL OF A DIAPHRAGM-TYPE CHLOR-ALKALI CELL

by PETER GAVIN COOK

A dissertation submitted to the Faculty of Engineering,
University of the Witwatersrand, Johannesburg,
for the degree of Master of Science in Engineering

Johannesburg 1978

DECLARATION

I, Peter Gavin Cook, declare that this dissertation is my own work and has not been submitted for a degree to any other University.

ABSTRACT

Experiments were performed on a small scale diaphragm-type chlor-alkali cell. The experimentation consisted of running the cell under conditions similar to those found in industrial cells. Steady-state flow runs were performed at various current densities and inlet flow rates. Concentrations of the various ions in the catholyte and anolyte were measured and mass and energy balances were performed.

A model of the chlor-alkali cell, based on the theory of the flux of an ion under potential, concentration and flow gradients as well as the kinetics of the electrode and bulk reactions, was developed. This model was tested against data found by experiments performed on the small-scale chlor-alkali cell.

Experiments for the characertisation of different diaphragms were also performed. These were: (i) pressure drop as a function of flow rate, (ii) diffusion of the sodium ion across a diaphragm, and (iii) physical geometry of a diaphragm. Four different woven diaphragms were investigated. The following trends were found: (i) at a given flow rate, the pressure drop across a diaphragm increased with decreasing void fraction, and (ii) the diffusion coefficient of the sodium ion increased with increasing void fraction.

ACKNOWLEDGEMENTS

I would first like to thank Professor Bryson for his great help with the dissertation, as well as all the members of the Department of Chemical Engineering for their readiness to discuss and help with any problems that arose; secondly, the workshop staff for building the sets of apparatus used.

I would also like to thank AECI for their study grant. Milton Buchalter was of great help in the earlier part of the research work in the design of the cell. Dr. D. Davies, of AECI Analytic Section, helped me solve many of my chemical analysis problems as well as doing various tests for me.

Mr. N. Webb for the photographs used in the dissertation.

Filtaflo for supplying the diaphragms used throughout the experimentation.

Permelec S.p.A. Milan, for supplying the anode.

Last, but not least, I would like to thank Mrs. C. Gross for the typing of this dissertation.

LIST OF SYMBOLS USED

Subscripts 0, 1, 2, 3, 4, refer respectively to H_2O, Na^+, Cl^-, OH^-, ClO^-

a	Surface area to unit volume ratio of screen (m^{-1})
a_i	anolyte concentration of species i (mole/litre)
A	Total diaphragm area (cm^2)
B	Screen thickness (m)
c_i	Concentration of species i (mole/litre)
cp_j	Heat capacity at constant pressure of stream j (cal/g° C)
c_T	$\sum c_i$ = total concentration including solvent (mole/litre)
d_s	Diameter of shute wire (m)
d_w	Diameter of warp wire (m)
D	Screen pore diameter (m)
D_i	Diffusion coefficient of species i (cm^2/s)
D_{ij}	Diffusion coefficient allowing for interaction between species i and j (cm^2/s)
e	Constant in equation 2.27
E	Electrostatic potential (V)
f	Friction factor
f_i	Concentration of species i in feed (mole/litre)
F	Faraday number = 96500 (coulombs/equiv.)
h_3 - h_8	Constants in equations 2,26 and 2,27
i	Current density (amp/cm^2)
i_2	Current density producing oxygen (amp/cm^2)
I	Current (amp)
k	Dissociation constant
K	Conductivity of solution (mho/cm)
K_{ij}	Friction or interaction coefficients (joule sec./cm^5)
l	Diaphragm thickness (cm)
l_{1s} , l_{2s}	Length of shute wire segment (m)
L	Fluid path length (m)
m_1	Concentration of NaCl (mole/kg.H_2O)
m_j	Mass flow rate of stream j (g/s)
Ma	Mass lost over anolyte (g/s)
Mc	Mass lost over catholyte (g/s)
M	Concentration of NaCl (mole/litre)
M_f	Mass flow rate of feed (g/s)
N	Concentration of NaOH (mole/litre)
N_i	Flux of species i (mole/sec. cm^3)
N_s	Number of shute wires (wires/m)
N_w	Number of warp wires (wires/m)
p	Pressure in fluid (cmH_2O)
p_a	Vapour pressure of water over anolyte (mmHg)
p_c	Vapour pressure of water over catholyte (mmHg)
p_o	Vapour pressure of pure water (mmHg)
Q_1 - Q_7	Heat content of streams 1 - 7 in energy balance (cal./sec.)
Q_d	Volume flow rate through diaphragm (cm^3/s)
Q_i	Volume flow rate into cell (cm^3/s)
Q_o	Volume flow rate out of cell (cm^3/s)

R_i	Production rate of species i (mole/cm^{3}s)
R	Universal gas constant = 8,314 (joule/mole°K)
t	Temperature (°C)
t_i	Transport or transference number of species i
t_1	Temperature of cell inlet (°C)
t_2	Operating temperature of cell (°C)
T	Temperature (°K)
u	Fluid approach velocity (cm/s)
u_i	Mobility of species i (cm^2 mole/joule sec.)
U	Overall heat transfer coefficient (watt/m^2 °C)
v	Fluid velocity (cm/s)
v_{ij}	Average velocity of species i, j (cm/s)
V	Voltage of cell (v)
Vo	Volume (cm^3)
w_1	Concentration of NaCl (weight %)
w_2	Concentration of NaOH (weight %)
x	Direction perpendicular to diaphragm
Z_i	Charge of species i

Greek Symbols

α	Viscous resistance coefficient
β	Inertial resistance coefficient
ϵ	Volume void fraction
Φ	Electrostatic potential (V)
Π	Atmospheric pressure (mmHg)
ρ	Fluid density (g/cm^3)
τ	Time (sec.)
μ	Fluid viscosity (c.poise)
μ_i	Electrochemical potential of species i (joule/mole)
ζ_A	Anodic current efficiency

LIST OF FIGURES

Figure No.		Page
1	Plot of OH^- transport number as a function of concentration	12
2	Logic diagram of the program for the model	17
3	Apparatus for measuring pressure drop across diaphragm	20
4	Apparatus for measuring pressure drop across diaphragm	22
5	Apparatus for measuring the diffusion of an ion through a diaphragm	23
6	Apparatus to measure diffusion coefficients at elevated temperatures	25
7	Plot of $\Delta p/u$ vs. u – Run 1	26
8	Plot of $\Delta p/u$ vs. u – Run 2	27
9	Plot of $\Delta p/u$ vs. u – Run 3	28
10	Plot of $\Delta p/u$ vs. u – Run 4	29
11	Plot of ln Δc vs. time – Run 1	31
12	Plot of ln Δc vs. time – Run 2	32
13	Plot of ln Δc vs. time – Run 3	33
14	Plot of ln Δc vs. time – Run 4	34
15	Plot of diffusion coefficients of Na^+, OH^- and Cl^- as a function of temperature	36
16	Chlor-alkali experimental cell	38
17	Experimental layout for the chlor-alkali cell	39

LIST OF TABLES

Table No.		Page
1	Typical operating conditions of a diaphragm-type chlor-alkali cell	2
2	*Diffusion coefficients of* Na^+ through different diaphragms	30
3	*Physical properties of diaphragm type 4*	30
4	Comparison of values found by experimentation and values predicted from model for the chlor alkali cell – a typical run	41
5	Summary of variables that the model predicts, their range and the error between predicted and experimental values	42

CONTENTS

1 Introduction 1
1.1 *Diaphragm-type* Chlor-Alkali Cells 1
1.1.1 The Diaphragm 2
1.1.2 The Electrodes 3
1.2 *Reactions Taking Place* in the Chlor-Alkali Cell 3
1.3 The Transport of Ions in Solution 5
1.3.1. Dilute Solution Theory 5
1.3.2. *Concentrated Solution Theory* 6
1.4 Modelling of Diaphragm type Chlor-Alkali Cell 6
1.4.1 Statistical Approach 7
1.4.3 Mechanistic Approach 7

2. Mathematical Model of a Diaphragm-type Chlor-Alkali Cell 9
2.1 Reaction Scheme 9
2.2 *Transport of Ions* through the Diaphragm 9
2.2.1 Modified Flux Equation 10
2.2.2 Calculation of OH^- Back Migration 11
2.3 Mass and *Component Balances* 11
2.4 Calculations of the Density and Vapour Pressure of the Solution, and the Transport Number of the Sodium Ion 13
2.5 Energy Balance 15
2.6 Logic Diagram of the Model 16

3. Preliminary Experimentation 19
3.1 *Introduction* 19
3.2 Characterisation of Diaphragm 19
3.2.1 Pressure drop across Diaphragm 19
3.2.2 *Diffusion of an* Ion through a Diaphragm 21
3.2.3 Geometry of the Physical Components of a Diaphragm 21
3.3. Diffusion coefficients of Na^+, Cl^- and OH^- at Elevated Temperatures 21
3.4 *Results and Discussion* 24
3.4.1 Characterisation of Diaphragm 24
3.4.2 Diffusion Coefficients at Elevated Temperatures 35

4 Experiments on Chlor-Alkali Cell 37
4.1 Details of Apparatus 37
4.2 Experimental Procedure 37

5. Results, Discussion and Conclusion 41

6. References 44

7 Appendix 45
7.1 Types of *Diaphragms used* 45
7.2 Theory for Pressure Drop Experiments 46
7.3 Theory for Diffusion of an Ion across a Diaphragm 47
7.4 *Equations for* Calculating Diaphragm Geometric Properties 48
7.5 Readings from Pressure Drop Experiments 50
7.6 Readings from Diffusion Experiments 51
7.7 Photomicrographs of Diaphragm Type 4 53
7.8 Measurements of the Physical Components of a Diaphragm 54
7.9 Methods of *Analysis for* Na^+, Cl^- and OH^- 56
7.10 Readings of diffusion Experiments at Elevated Temperatures 57
7.11 Readings from Runs Performed on the *Chlor-Alkali Cell* 59
7.12 Chlor-Alkali Cell - Logic Diagram of Mass Balance 63
7.13 Comparison of Experimental Results and those Predicted by the *Model for the Chlor-Alkali Cell* 64
7.14 Fortran Program of Model 67

1. INTRODUCTION

The demand for chlorine and caustic soda has been growing over the past thirty years, consequently plant capacity has had to be scaled up and new designs developed. The average annual growth rate for the United States of America as far back as the decade 1950 - 1969 was 8%.[1] The largest producers of chlorine and caustic soda in 1972 were:[2] U.S.A. with an annual caustic soda tonnage of 9,4 million, Japan with 3,6 million, West Germany with 2,2 million and Canada, Italy and France with about 1,0 million tons.

The two major processes used in chlorine-caustic production are the mercury process and the diaphragm process. The mercury process is favoured in most of the countries mentioned above, with the U.S.A. and Canada being two where the diaphragm process is predominantly used. The reasons for this are the supply situation of the raw material salt and the market structure concerning the products. In the U.S.A. and Canada, natural brine is used as the raw material and a high purity caustic soda is not required so the diaphragm process suffices. In Japan especially, and some of the other chlorine producing countries, the raw material is rock salt so the mercury process is more economical. Added to this is the fact that the caustic soda consumers demand a high purity product for use in the chemical fibre industry. About 60% of the chlorine produced in 1971 was used in the plastics industry, chiefly for P.V.C. production.[1]

The mercury process has some advantages over the diaphragm process, these are: (i) the product caustic soda is concentrated and hence meets any consumer requirements, and (ii) a smaller capital investment is required to produce the same quantity of chlorine and caustic soda because of the higher current densities used.

On the other hand the mercury process not only uses large quantities of mercury but also has a major problem in the form of environmental pollution. One example of such pollution is the high concentration of mercury found in fish caught in the Japan Sea. As a direct result of this there has been over the last few years a swing towards the diaphragm process. With improved technology and the increasing awareness of the world towards environmental pollution, the diaphragm process should soon become the major process used in chlorine and caustic soda manufacture.

1.1 Diaphragm-type Chlor-alkali cells

In Table 1 typical operating conditions and dimensions of a cell are given.[2]

The typical cell consists of an arrangement of anode-diaphragm-cathode-anode-etc. and the typical chlor-alkali plant consists of 100 to 150 of these cells connected electrically in series.[3]

The brine, at an inlet concentration of around 300 g/l NaCl and a temperature of 50 - 80°C, is fed into the anode compartments. Here it undergoes electrolysis and flows through the diaphragm into the cathode compartments. The chlorine is collected over the anode compartments and the hydrogen over the cathode compartments. The spent brine/caustic solution flows out of the cathode compartments and the caustic is con-

TABLE 1

Current capacity	75kA
Mean cell voltage	3,63v
Current efficiency	96,5%
Anode material	D.S.E.*
Cell dimensions	1,7x1.84x1.88m
D.C. power consumption	2,521kWhr/ton NaOH
Catholyte concentration	130 - 140g/l NaOH
Life of diaphragm	180 - 360 days

* Dimensionally Stable Electrode

centrated by means of a double- or triple-effect vacuum evaporator.

The basic reactions that take place are : (i) at the anode Cl^- is discharged and chlorine gas is evolved, and (ii) at the cathode H^+ is discharged and caustic soda as well as hydrogen gas are formed. The following side reactions also take place : chlorine gas and caustic soda react to form sodium hypochlorite and chlorate, and oxygen is liberated by the electrolytic decomposition of water.

In order to minimise these unwanted side reactions, the porous diaphragm is used to separate anolyte from catholyte. The diaphragm must at the same time allow transmission of electric current, i.e. it should be ion permeable. The diaphragm restricts the transport of the OH^- ion from catholyte to anolyte as well as preventing the mixing of the chlorine and hydrogen gases.

1.1.1. The Diaphragm

Conditions in chlor-alkali cells are such that diaphragms must be resistant to chlorine attack in acid and alkali conditions at temperatures up to 100°C. The only material used in commercial diaphragms is asbestos. Depending on the type of cell, electrode, and raw material the diaphragms can be made from asbestos fabric, paper or fibre, the latter being the most common. The life of the diaphragm can vary from 90 - 400 days.[2]

A brief description of the manufacture of a diaphragm from asbestos fibres is as follows:[4] Asbestos fibres are dispersed in an aqueous solution using a pulper. The concentration of the asbestos is 1 - 10% by weight and the aqueous solution contains a water soluble thickening agent of surface active character (a non-biodegradable synthetic resin). The diaphragm support takes the form of a perforated plate which also acts as the cathode. The aqueous asbestos slurry is sucked through the diaphragm support depositing the asbestos fibres. When the asbestos has been deposited to the desired thickness the diaphragm plus support are baked to set and harden the fibres.

1.1.2. The Electrodes [1, 2, 5]

Over the last few years the material of construction of the anode has been undergoing great changes. Although graphite anodes are still being used commercially to some extent, metal anodes are now starting to capture the market. The cathode is made from steel mesh and has none of the problems associated with the anode because of the alkalinity of the solution and the absence of chlorine.

If graphite electrodes are used they are consumed during electrolysis and have lives of 180 - 200 days. Research by Nippon Carbon[2] has developed graphite anodes with a greater corrosion resistance and life expectancies of 6 - 15 months. In order to optimise the operation of the cell the anode to cathode gap has to be adjusted and this together with the blocking of the diaphragm with graphite particles are the main disadvantages of these anodes.

The new metal anodes are called 'permanent' or 'dimensionally stable electrodes' because they are non-consumable. Research and development work has concentrated on two main types: (i) titanium electrodes coated with noble metals of the platinum group (especially Pt, Pd, Ir, Rh), and (ii) titanium electrodes coated with oxides of noble metals (especially Ru, Ir). These new anodes have the advantage that they can be obtained in the expanded metal form, which facilitates the brine flow and the chlorine liberation in the cells.

1.2. Reactions taking place in the chlor-alkali cell

The reactions can be classified into anodic, cathodic and bulk reactions.

The main anodic reaction on a 'Dimensionally Stable Electrode' is the oxidation of chloride ions:

$$2Cl^- \rightarrow 2Cl(ads) + 2e^- \qquad 1A$$
$$2Cl(ads) \rightarrow Cl_2 \qquad 1B$$

The above two equations are the scheme by which chlorine is evolved[1] with equation 1A being the rate determining step.[5]

The main anodic side reaction is the evolution of oxygen:

$$2H_2O \rightarrow O_2 + 4H^+ + 4e^- \qquad 1C$$

Simultaneous oxygen evolution and chlorate formation may also take place by an electrode reaction:[6, 7, 8]

$$6ClO^- + 3H_2O \rightarrow 6H^+ + 2ClO_3^- + 4Cl^- + 3/2\,O_2 + 6e^- \qquad 1D$$

The oxidation of chlorate to perchlorate is possible on electrodes which have a high oxygen overvoltage but is negligible on graphite and metal electrodes.

$$ClO_3^- + H_2O \rightarrow ClO_4^- + 2H^+ + 2e^- \qquad 1E$$

The main cathodic reaction is the *reduction of water to evolve* hydrogen;

$$2H_2O + 2e^- \rightarrow H_2 + 2OH^- \qquad 1F$$

Side reactions that also occur on the cathode are the reduction of chlorate and hypochlorite:

$$ClO_3^- + 3H_2O + 6e^- \rightarrow Cl^- + 6OH^- \qquad 1G$$
$$ClO^- + H_2O + 2e^- \rightarrow Cl^- + 2OH^- \qquad 1H$$

The reduction of hypochlorite is well documented,[6] and equation 1H goes almost to completion, while equation 1G is much slower.[6] *Hine and Yasuda*[7] *concluded* that the *charge transfer* of ClO^- is fast and that the cathodic reduction of ClO_3^- (reaction 1G) may not take place under the operating conditions found in commercial chlor-alkali cells.

The *reactions* taking place in the bulk electrolyte are:[7, 8]

$$Cl_2\,(g) \rightleftharpoons Cl_2\,(aq) \qquad 1I$$
$$Cl_2\,(aq) + H_2O \rightleftharpoons HClO + Cl^- + H^+ \qquad 1J$$
$$HClO \rightleftharpoons H^+ + ClO^- \qquad 1K$$
$$2HClO + ClO^- \rightarrow ClO_3^- + 2H^+ + 2Cl^- \qquad 1L$$

The reactions 1I to 1L take place in the anode compartment of *the cell. Reactions 1I to 1K are considered to be at equilibrium* and reaction 1L, the chemical chlorate formation, is too slow to reach equilibrium.

The *chemical* reduction of hypochlorite occurs in the catholyte:[9]

$$ClO^- + H_2 \rightarrow Cl^- + H_2O \qquad 1M$$

Very little experimental work has been done on the kinetics of the electrochemical reactions *under conditions experienced in* chlor-alkali cells. Faita and Fiori,[5] Cerquetti, Longhi, Mussini and Natta,[10] as well as Bianchi[1] have done some work on the electrochemical reactions on 'Dimensionally Stable Electrodes'. Nagy[9] has summarised *most of* the known *kinetic data and he gives the following* expressions:

$$[HOCl] = \exp(-13{,}8385 - 2{,}30259\times10^{-3}\times t + 5.92106 \times 10^{-2} \times [NaCl] + 2.30259 \times pH) \qquad 1.1$$

The dissociation constant for reaction 1K can be expressed *as:*

$$k = 3{,}7508 \times 10^{-6} \exp(-1450{,}6/T) \qquad 1.2$$

The chlorate production rate can be found from:

$$\frac{d[NaClO_3]}{d\tau} = 5{,}555 \times 10^{-3} \exp(0{,}6 + 0{,}056 \times t) \times [HOCl]^2 \times [OCl^-] \qquad 1.3$$

...e transport of ions in solution[11]

1.3.1. Dilute solution theory

The flux of each ionic species may be expressed as:

$$N_i = -Z_i u_i F c_i \nabla \Phi \quad - D_i \nabla c_i + c_i v \qquad 1.4$$

In this equation N_i is the flux of a species i and indicates the direction and rate of movement of the species. The three terms on the right represent the three mechanisms of mass transfer: (i) motion of a charged species in an electric field, (ii) molecular diffusion due to a concentration gradient and (iii) convection due to the bulk motion of the solution.

The current density in the solution can be expressed in terms of the fluxes of all the species:

$$i = F \sum_i Z_i N_i \qquad 1.5$$

The material balance for each species is:

$$\frac{\partial c_i}{\partial \tau} = - \nabla N_i + R_i \qquad 1.6$$

Where R_i is the production rate of the ith species.

All electrolytic solutions are electrically neutral except in a thin layer near the electrodes, hence in the bulk solution:

$$\sum_i Z_i c_i = 0 \qquad 1.7$$

Equations 1.5 and 1.6 are basic physical laws and equation 1.7 is an 'accurate assumption'.[11] The only doubtful equation is equation 1.4, the flux equation. The driving force for diffusion should be an activity gradient and activities are equivalent to concentrations only for extremely dilute solutions. The bulk flow of a species, v, is only equal to the bulk solution velocity for dilute solutions.

Hence it can be seen that although equation 1.4 is used extensively in electrochemistry it must be used cautiously and can only be applied in certain cases.

Combining equations 1.4 and 1.5:

$$i = -F^2 \nabla \Phi \sum_i Z_i^2 u_i c_i - F \sum_i Z_i D_i \nabla c_i + Fv \sum_i Z_i c_i \qquad 1.8$$

from equation 1.7 the last term is zero and for the case of no concentration variations:

$$i = K\nabla\Phi \qquad 1.9$$

where $K = F^2 \sum_i Z_i^2 u_i c_i$ and is the conductivity of the solution.

The fraction of the current carried by species j, $t_j x i$, can be written for the case of no concentration variations:

$$t_j \times i = -F^2 Z_j^2 u_j c_j \nabla\Phi = \frac{Z_j^2 u_j c_j}{\sum_i Z_i^2 u_j c_j} \times i \qquad 1.10$$

Hence $t_j = \frac{Z_j^2 u_j c_j}{\sum_i Z_i^2 u_j c_j}$ and is called the transference or transport number.

The Nernst-Einstein equation provides a relationship between D_i, the diffusion coefficient, and u_i, the mobility, of a species i:[11]

$$D_i = RTu_i \qquad 1.11$$

1.3.2. Concentrated Solution Theory

Equation 1.4, section 1.3.1., should for concentrated solutions be replaced by:[11]

$$c_i \nabla\mu_i = \sum_j K_{ij}(v_j - v_i) = RT \sum_j \frac{c_i c_j}{c_T D_{ij}} \qquad 1.12$$

Where μ_i is the electrochemical potential of species i, K_{ij} is the friction or interaction coefficient.

D_{ij} is a 'diffusion coefficient' allowing for interaction between species i and j, and v_i, v_j are the average velocities of species i and j.

The development of the concentrated solution theory for use in this thesis will be dealt with in section 2.2.

1.4. Modelling of diaphragm-type cells

The modelling of electrochemical systems, as with many other systems, can be carried out in two ways. The statistical approach which is based on data obtained from operating plants, this data is fitted to equations with adjustable parameters – hence the model is forced to fit the experimental data. The mechanistic approach, on the other hand, is based on the understanding of the physical, chemical and electrical processes taking place.

Both approaches have their advantages and disadvantages. The statistical approach, because of the data used, is limited to a narrow range in the operating variables and hence extrapolation could lead to errors. The mechanistic approach usually necessitates over-

simplification so that the model can be solved mathematically. Due to the lack of physical and chemical data further assumptions and the incorporation of adjustable parameters may have to be resorted to.

1.4.1. Statistical Approach

MacMullin[3] has developed a model of a graphite anode diaphragm cell using the statistical approach. Variables considered by MacMullin were: anode wear, gas hold-up, velocity of solution in anode-diaphragm gap, and the changing conductivity of the asbestos diaphragm.

The basic logic diagram of the model took the following form: (i) the cell temperature and the anolyte salt concentration were assumed, (ii) the mass balance over the anolyte compartment was performed, (iii) an iterative scheme was performed around the salt concentration in the anolyte, (iv) the energy, and the overall mass balance were then performed, (v) the final loop was iterated around the assumed and calculated temperatures.

This model was fitted to data taken from an industrial chlor-alkali plant. The model can be used to predict current efficiency, anolyte concentrations, catholyte concentrations, amounts of chlorine, oxygen and hydrogen production, cell voltage, days remaining to anode and diaphragm changes, and the power used per ton of chlorine produced.

1.4.2. Mechanistic Approach

Nagy[9] has recently published a paper on a mechanistic type model for a diaphragm chlor-alkali cell. The reaction scheme used by Nagy was very similar to the reactions given in section 1.2. Nagy used the flux equation for dilute solutions leaving out the diffusion term. He showed that this term was only a few percent of the total mass flux. This is valid for most practical situations, but the diffusion and electrical migration terms have approximately equal magnitudes – hence there is no reason, other than simplifying the mathematical solution, for retaining one of the terms and leaving out the other.

The input into Nagy's model included the OH^- back migration rate and the cell temperature as well as inlet flow rates, concentrations and cell dimensions. The cell temperature and the OH^- back migration rate will generally not be known when one wishes to predict the behaviour of a chlor-alkali cell under differing inlet conditions. The calculation procedure for the model took the following form: (i) the oxygen production rate and the anolyte salt concentration were assumed, (ii) the program iterated around the salt concentration, (iii) the pH of the anolyte was assumed, (iv) the program then iterated around the pH value, (v) an iterative procedure was then performed about the assumed oxygen production rate, (vi) the catholyte concentrations of salt and caustic were assumed and an iterative procedure was performed about these.

A more general type of mechanistic model should incorporate means to calculate the

cell temperature and the OH^- back migration rate. The latter being of great importance as it gives a direct estimate of the anodic current efficiency.

2. MATHEMATICAL MODEL OF A DIAPHRAGM-TYPE CHLOR-ALKALI CELL

The model derived in this thesis follows quite closely the one proposed by Nagy.[9] The areas where it deviates will be pointed out.

The overall assumption made in the model is one of steady-state cell operation. A further assumption is that the anolyte and catholyte are both well mixed due to gas evolution. Under these conditions, concentration gradients in the bulk solution will be small, and so one can assume that the cell outlet will have the same concentration as the catholyte.

2.1. Reaction Scheme

All the reactions taking place in a chlor-alkali cell have already been discussed in section 1.2, and are reactions 1A through 1M. Their rates depend on the concentrations of the various chemical species, the electrode material, and the temperature. The equilibrium constants and expressions used in the model are given in section 1.2.

In order to simplify the reaction scheme and hence the determination of the mass balance, it is assumed that a relatively small amount of chlorate is formed. The reaction scheme that will be considered consists of the following electrode reactions:

$$2Cl^- \longrightarrow Cl_2 + 2e^- \qquad 2A$$

$$2H_2O \longrightarrow O_2 + 4H^+ + 4e^- \qquad 2B$$

$$2H_2O + 2e^- \longrightarrow H_2 + 2OH^- \qquad 2C$$

The liberation of chlorine, equation 2A, takes place with an anodic efficiency of ζ_A. Oxygen liberation is the only competing process considered at the anode and will result in a $\zeta_A < 1$. Hydrogen is liberated at the cathode with an efficiency of ζ_C. For all calculations in this thesis the only cathode reaction considered is 2C and hence it is assumed that $\zeta_C = 1$.

The assumption of negligible chlorate production was shown to be reasonable once analysis of the anolyte and catholyte had been performed. The chlorate and hypochlorite concentrations were found to be typically two hundred times less than the sodium, chloride and hydroxyl concentrations in anolyte and catholyte.

2.2. Transport of ions through the diaphragm

The concentrations found in a chlor-alkali cell are typically in the order of 4 - 5 molar for sodium chloride, and 2 - 3 molar for sodium hydroxide. These are far from dilute solutions and hence one must consider the concentrated solution theory for deriving the flux equation.

If one considers the flux in only one direction, i.e. perpendicular to the plane of the diaphragm, and calls that the x-direction, one can write:[11]

$$c_i \frac{d\mu_i}{dx} = RT \sum_j \frac{c_i c_j}{c_T D_{ij}} (v_j - v_i) \qquad 2.1$$

If the solvent, water, is assigned the subscript 0 and Na^+, Cl^- and OH^- are represented by subscripts 1, 2 and 3 respectively, then one can remove j = 0 from the summation in *equation* 2.1 as follows:

$$c_i \frac{d\mu_i}{dx} = RT \frac{c_i c_o}{c_T D_{io}} (v_o - v_i) + RT \sum_{j=1} \frac{c_i c_j}{c_T D_{ij}} (v_j - v_i) \qquad 2.2$$

Now since the concentration of the solvent, water, is approximately 55 molar and the concentrations of the other ions are in the range 2 - 6 molar, one can make the following assumptions. (i) c_i/c_o is small, for i > 0; (ii) $C_o \simeq C_T$. Therefore in equation 2.2 the first term on the right hand side is *approximately an order of magnitude* larger than the second term provided the D_{ij} values for j > 1 are of similar magnitude to D_{io}, hence:

$$c_i \frac{d\mu_i}{dx} \simeq \frac{RTc_i}{D_{io}} (v_o - v_i) \qquad 2.3$$

The next assumption made is that μ_i, the electrochemical potential, can be expressed as the sum of the electrical and chemical potentials:

$$\mu_i = \mu_i^o + Z_i F(E - E^o) + RT \ln \frac{c_i}{c_o} \qquad 2.4$$

This also satisfies the Nernst-Einstein relation. Using equations 2.3 and 2.4 as well as the Nernst-Einstein relation one can write:

$$N_i = c_i v_i = -u_i c_i Z_i F \frac{dE}{dx} - D_{io} \frac{dc_i}{dx} + c_i v_o \qquad 2.5$$

We see therefore that for solutions containing up to 6 molar concentrations of salt, the form of the flux equation can be approximated to that *for dilute solutions.*

2.2.1 Modified flux equation

In the flux equation one wants to *eliminate the potential gradient* $\frac{dE}{dx}$, as it is difficult to measure and does not have any real meaning when a concentration gradient exists.[11] Multiplying equation 2.5 by Z_i and summing:

$$\sum_i Z_i N_i = -\sum_i u_i c_i Z_i^2 F \frac{dE}{dx} - \sum_i Z_i D_{io} \frac{dc_i}{dx} + \sum_i Z_i c_i v_o \qquad 2.6$$

The last term is zero from electroneutrality. Eliminating $\frac{dE}{dx}$ between the equations 1.5 and 2.6.

$$N_i = \frac{it_i}{Z_i F} + \frac{t_i}{Z_i} \sum_j Z_j D_{jo} \frac{dc_j}{dx} - D_{io} \frac{dc_i}{dx} + c_i v_o \qquad 2.7$$

The form of equation 2.7 is similar to that of the original flux equation. The first term describes the motion of species i due to the electric field, while the second term accounts for the motion of species i due to a potential caused by the concentration gradients.

2.2.2. Calculation of OH^- back migration

The calculation procedure used in section 2.6 requires that the OH^- back migration rate be calculated. The OH^- flux, N_3, can be calculated from equation 2.7 provided the value of t_3, the hydroxyl transport number, is known. As experimental values of this quantity could not be found in the literature, it was decided to measure the flux on the experimental cell under a variety of operating conditions and to attempt to correlate it with catholyte composition. From equation 2.7, t_3 can be expressed as:

$$t_3 = \frac{N_3 - D_{30}\left(\frac{dc_3}{dx}\right)^* + c_3^* v_0}{\frac{i}{F} - \sum_i Z_i D_{i0}\left(\frac{dc_i}{dx}\right)^*} \qquad 2.8$$

where c_3^* is the arithmetic average concentration between anolyte and catholyte and $\left(\frac{dc_i}{dx}\right)^*$ is taken as the difference in concentration between catholyte and anolyte divided by the diaphragm thickness. The values of t_3 thus obtained are plotted as a function of c_3 in fig. 1. The experimental points fall very nearly on a straight line and the following expression is obtained using the method of least squares:

$$t_3 = -258{,}26c_3 + 0{,}59 \qquad 2.9$$

This expression shows that t_3 decreases with increasing c_3 and that negative transport numbers can be obtained for $c_3 > 2.15$ molar. This is possibly due to interaction between ions where the assumptions made in section 2.2 are not entirely justified for the OH^- ion. Equation 2.9 is therefore an empirical relationship, where the numerical coefficients have to be fitted experimently.

2.3 Mass and component balances

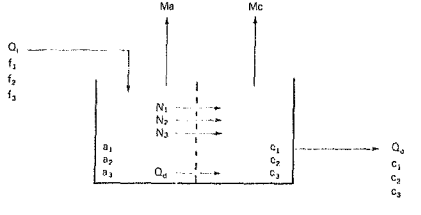
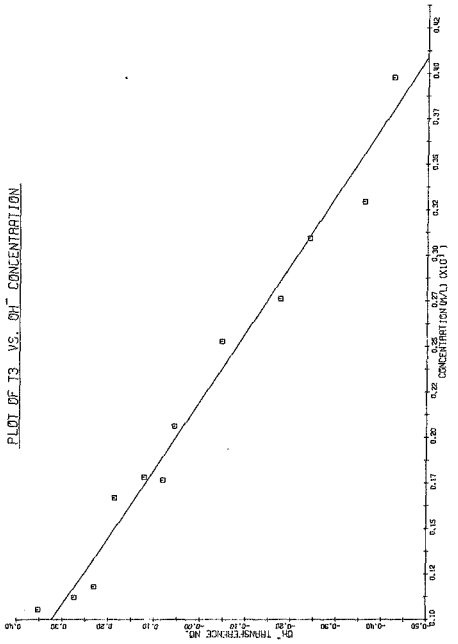


FIGURE 1.


PLOT OF T3 VS. OH⁻ CONCENTRATION
OH⁻ TRANSMITTANCE NO.
CONCENTRATION(M/L) (X10⁻¹)

Subscripts 1, 2, 3 refer to Na^+, Cl^- and OH^-; f, a, and c refer to the feed, anolyte and catholyte concentrations.

Anode compartment component balances:

$$Q_f f_1 = N_1 A \qquad 2.10$$

$$Q_f f_2 = N_2 A - \frac{t_A I}{F} \qquad 2.11$$

$$Q_f f_3 = N_3 A + \frac{(1 - t_A) I}{F} \qquad 2.12$$

Cathode compartment component balances:

$$N_1 A = Q_a c_1 \qquad 2.13$$

$$N_2 = Q_a c_2 \qquad 2.14$$

$$N_3 = Q_a c_3 - \frac{I}{F} \qquad 2.15$$

Overall component balances:

$$Q_f f_1 = Q_a c_1 \qquad 2.16$$

$$Q_f f_2 = Q_a c_2 - \frac{t_A I}{F} \qquad 2.17$$

$$Q_f f_3 = Q_a c_3 - \frac{I}{F} \qquad 2.18$$

Mass balances:

Anode:	$\rho_f Q_f = \rho_a Q_a + Ma$	2.19
Cathode:	$\rho_f Q_a = \rho_c Q_a + Mc$	2.20
Overall:	$\rho_f Q_f = \rho_c Q_a + Ma + Mc$	2.21

Where Ma and Mc are the total masses lost over anolyte and catholyte.

2.4 Calculations of the density and vapor pressure of the solutions, and the transport number of the sodium ion.

In order to perform the mass balance one needs estimates of: (i) densities of the feed, anolyte and catholyte as functions of concentration and temperature, (ii) the water lost with the gases over the anolyte and catholyte, and (iii) the sodium ion transport number.

Nagy[9] gives algorithms for calculating the densities of the different solutions.

NaCl solution: $p_1 =$ $1{,}0004075 - 7{,}1687895\times10^{-6}\,xt - 5{,}1792075\times10^{-6}\,xt^2 + 1{,}054032\times10^{-8}\,xt^3 + (7{,}4569085\times10^{-3} - 2{,}960572\times10^{-5}\,xt + 3{,}0504225\times10^{-7}\,xt^2 - 9{,}3493315\times10^{-10}\,xt^2)\,xw_1 + (1{,}8372605\times10^{-5} + 4{,}2360185\times10^{-7}\,xt - 5{,}1483125\times10^{-9}\,xt^2 + 1{,}794537\times10^{-11}\,xt^3)\,xw_1^2$ 2.22

NaCl/NaOH solution: $p_2 =$ $1{,}00686 + 1{,}147527\times10^{-2}\,xw_2 - 1{,}722033\times10^{-5}\,xw_2^2 - 3{,}585138\times10^{-4}\,xt - 2{,}143812\times10^{-6}\,xt^2 + 7{,}550802\times10^{-3}\,xw_1$ 2.23

Where w_1 and w_2 are the weight percent concentrations of NaCl and NaOH respectively.

MacMullin[12] gives algorithms for the vapor pressure of water over aqueous solutions of salt and caustic soda. The gas mixtures above anolyte and catholyte are assumed to be ideal. The deviation from ideality of the major components is less than 1% at 1 atmosphere and 90°C.[9]

Anode compartment:

(i) NaCl concentration > 3 molar:

$$p_a = (1-((M-3)(1{,}9772\times10^{-3} - 1{,}193\times10^{-5}\,xt) + 0{,}035)M)\,p_o \qquad 2.24$$

(ii) NaCl concentration < 3 molar:

$$p_a = (1-0{,}035M)\,p_o \qquad 2.25$$

Cathode compartment:

NaCl concentration > 3 molar and NaOH concentration < 12,5 molar.

$$p_c = (1-((M-3)(1{,}9772\times10^{-3} - 1{,}193\times10^{-5}\,xt) + 0{,}035M - (\{174-t\}(h_1 + h_2N + h_3N^2 + \frac{h_4}{N}) + 0{,}0317)N)\,p_o \qquad 2.26$$

Where $h_1 = -8{,}6715\times10^{-5}$
$h_2 = 3{,}368\times10^{-5}$
$h_3 = -1{,}354\times10^{-6}$
$h_4 = 7{,}88\times10^{-5}$

The value of p_o, the vapor pressure of pure water, is also calculated by an algorithm given by MacMullin.[12]

$$p_o = 10^{\left[5{,}219603 - \frac{a}{T}\left(h_1 + h_2a + h_3a^3\right)\right]} \qquad 2.27$$

Where $e = 374,11 - t$

$h_5 = 3,2437814$

$h_6 = 5,86826 \times 10^{-3}$

$h_7 = 1,1762379 \times 10^{-8}$

$h_8 = 2,1878462 \times 10^{-3}$

The amount of water lost with the gases over the anolyte and catholyte can be calculated from:

$$\text{moles } H_2O \text{ lost} = (\text{moles of gas evolved}) \frac{p_4}{\Pi - p_a} \qquad 2.28$$

Where Π is the atmospheric pressure and is taken to be 630mm Hg for all calculations in the thesis.

Mussini and Pagella[13] have measured transport numbers of NaCl at various temperatures and concentrations and their results can be expressed as follows:

$$t_{NaCl} = 0,3754377 + 4,864677 \times 10^{-4} xt + (-0,03151785 + 1,455249 \times 10^{-4} xt) xm_1 + (0,011552 - 3,588446 \times 10^{-5} xt) xm_1^2 + (-1,297191 \times 10^{-3} + 3,044053 \times 10^{-6} xt) xm_1^3 \qquad 2.29$$

Where m_1 is the concentration of NaCl in moles/kgH_2O.

2.5 Energy Balance

An energy balance is performed over the cell for *all* the experimental runs. This yields values of the heat lost through the walls of the cell, and hence values of U, the overall heat transfer coefficient. Using this value of U, and knowing the inlet feed flow rate and temperature, t_1, the operating temperature, t_2, of the cell is calculated *iteratively* from:

$$t_2 = \text{Heat lost}/UA + 20 \qquad 2.30$$

Where A is the total surface area of the cell and the ambient air temperature is taken to be 20° C.

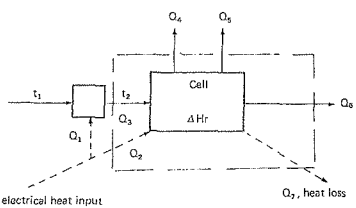
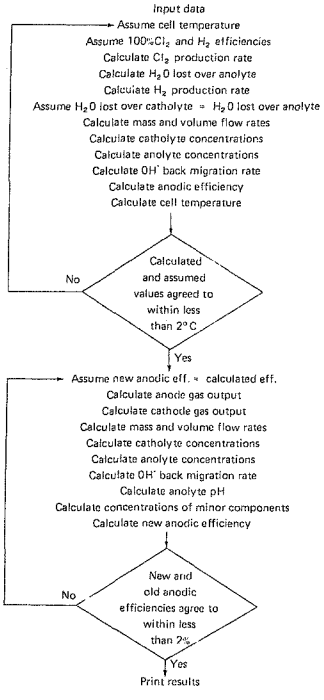


FIGURE 2


Input data
Assume cell temperature
Assume 100% Cl_2 and H_2 efficiencies
Calculate Cl_2 production rate
Calculate H_2O lost over anolyte
Calculate H_2 production rate
Assume H_2O lost over catholyte = H_2O lost over anolyte
Calculate mass and volume flow rates
Calculate catholyte concentrations
Calculate anolyte concentrations
Calculate OH^- back migration rate
Calculate anodic efficiency
Calculate cell temperature
Calculated and assumed values agreed to within less than 2°C
No
Yes
Assume new anodic eff. = calculated eff.
Calculate anode gas output
Calculate cathode gas output
Calculate mass and volume flow rates
Calculate catholyte concentrations
Calculate anolyte concentrations
Calculate OH^- back migration rate
Calculate anolyte pH
Calculate concentrations of minor components
Calculate new anodic efficiency
New and old anodic efficiencies agree to within less than 2%
No
Yes
Print results

of the model. This second section or main loop calculates all the desired values of the concentration, flow rates and efficiency.

In the first loop the anode and cathode efficiencies are assumed to be 100%. A cell temperature is assumed and the program then calculates the anode compartment gas output, i.e. the chlorine produced and the water vapor lost with it.

$$\text{Moles chlorine produced} = \frac{I\zeta_A}{F} \qquad 2.34$$

The moles of water lost are calculated according to equation 2.28. The cathode compartment gas output is then found. The water lost over the cathode compartment is assumed to be equal to that lost over the anode compartment. The mass and volume flow rates through the diaphragm and at the outlet are then computed. The salt and caustic concentrations in the catholyte are calculated from overall sodium and chloride balances. Using the modified flux equation (equation 2.7), the anolyte concentrations are found (the Na^+ concentration is assumed to be equal to the Cl^- concentration). In the modified flux equation a value of the transport number of sodium is needed, this is calculated from the algorithm given as equation 2.29. The OH^- back migration rate is then calculated from the flux equation using experimentally fitted values of t_3, the OH^- transport number (see section 2.2.2). The anode efficiency is computed from equation 2.11, i.e.:

$$\zeta_A = 1 + \frac{N_3 AF}{I} \qquad 2.35$$

At this stage the cell operating temperature is calculated using equation 2.30. This calculated value is compared to the initial assumed value and the initialising loop ends when the difference is less than 1,5°C.

The model now moves into its main loop. This loop is essentially very similar to the initialising loop, and starts with the cell temperature and an estimate of the anode current efficiency. Allowance is made for oxygen evolution which also alters the amount of water lost over the anode compartment. Since estimates of the catholyte concentrations are known from the initialising loop, the cathode gas composition can be calculated rather than assumed. The density of the catholyte can also be calculated – this improves the values obtained for the flow rates. The anolyte pH is then estimated from an expression derived by Nagy[9] for an experimental cell:

$$i_3 = (6{,}3115\times10^{-4} + 1{,}48291\times10^{-6}\times t - 1{,}61334\times10^{-4}\times M) \times 10^{0{,}62\times\exp(1{,}15129\times pH)} \qquad 2.36$$

where i_3 is the current density producing oxygen and is given by:

$$i_3 = \frac{(1-\zeta_A)I}{A} \qquad 2.37$$

Next, the concentration and production rate of the minor components, ClO^- and ClO_3^-, are calculated using equations given in section 1.2.4. The OH^- back migration and anode efficiency are calculated as in the first loop. The new calculated value of the anodic efficiency is compared to the old calculated value and the main loop is terminated when the difference is less than 2%.

3. PRELIMINARY EXPERIMENTATION

3.1 Introduction

The preliminary experimentation takes the form of two sections. In the first an attempt is made to characterise different diaphragms, and in the second diffusion coefficients of Na^+, Cl^- and OH^- are obtained as functions of temperature.

A diaphragm can be characterised by: (i) the pressure drop variation when a fluid flows through it at different rates, (ii) the transport, by molecular diffusion, of a soluble species due to concentration gradients, and (iii) the geometry of the physical components of a diaphragm as observed under the microscope.

Four different types of diaphragm are investigated in this thesis and their manufacturers' specifications are given in Appendix 7.1. All four diaphragms are woven filter-cloth type diaphragms.

Fluid flow through woven screens has been investigated by Armour and Cannon[15] and they treated this as being similar to flow through a thin packed bed. The pressure drop through the bed was considered to be the sum of viscous and inertial effects. The following relationship between pressure drop and fluid velocity was derived:

$$\frac{\Delta p\, \epsilon^2 D}{L \rho u^2} = \frac{(\frac{\alpha}{\rho u})}{u(a^2 D)} + \beta \qquad 3.1$$

where α and β are the viscous and inertial resistance coefficients, Δp is the pressure drop, ϵ is the void fraction, D is the pore diameter, L is the fluid path length, ρ is the fluid density, u is the fluid velocity, μ is the fluid viscosity, and A is the surface area to unit volume ratio of the diaphragm. Further details of the theory for the pressure drop experimentation is given in Appendix 7.2.

The diffusion of an ion across a diaphragm is in general dependant on: (i) concentration gradient, (ii) temperature, and (iii) the physical characteristics of the diaphragm. If one keeps the first two constant, then by changing the diaphragm one can observe the changes in the diffusion coefficient. The theory for the diffusion experimentation is given in Appendix 7.3. Only the transport of the sodium ion is investigated in this set of experiments.

Only one type of diaphragm is studied concerning the geometry of its physical components. This is type no. 4 which is the diaphram used in the experimental chlor-alkali cell. Equations expressing surface area to unit volume ratio, A, diaphragm thickness, B, and void fraction, ϵ, in terms of measurable variables are given in Appendix 7.4.

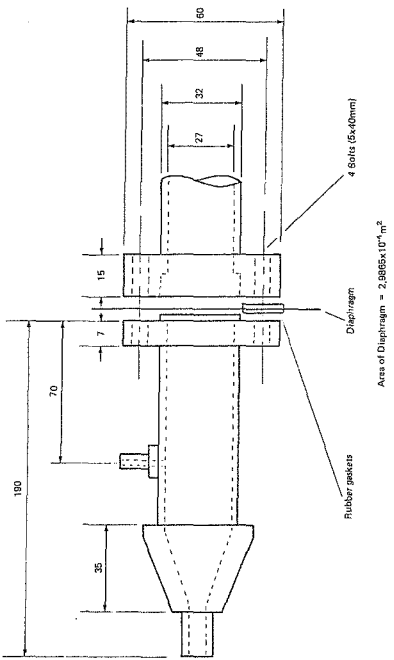
3.2 Characterisation of Diaphragm

3.2.1. Pressure drop across diaphragm

The apparatus consists of two pipe sections as shown in figure 3. The material of con-

FIGURE 3

Apparatus for measuring pressure drop across diaphragm
(All dimensions in mm)



struction is p.v.c. and the diaphragm is bolted between two flanges with a rubber gasket on either side of it. Tension is applied to the diaphragm when the bolts, holding the two sections together, are tightened. The pipe sections are connected to the remainder of the apparatus as shown in figure 4. Water is delivered from a constant level head tank and flows via a valve through the diaphragm, causing a pressure difference which is measured with an air-water manometer.

The experimental procedure is as follows. The diaphragm is bolted into position and the apparatus is connected as shown in figure 4. The system is filled with water and the air—water manometer is allowed to stabilise. The valve is opened and a series of readings are taken as the flow rate increases. Readings are also taken as the valve is closed in stages. At each reading sufficient time is allowed for the system to reach steady-state. The flow rate is measured using a stop watch and a measuring cylinder. Experiments were performed on the four types of diaphragm and the readings are reported in Appendix 7.5.

3.2.2. Diffusion of an ion through a diaphragm

The apparatus consists of two identical sections bolted together with the diaphragm and rubber gaskets inbetween as shown in figure 5. The bolts used are 3x30 mm brass bolts, and the material of construction is perspex.

The experimental procedure is as follows. The apparatus is bolted together with the diaphragm and gaskets in position. A measured volume of distilled water is poured into the cell and the levels on either side of the diaphragm are allowed to equilibrate. At a noted time, equal measured volumes of a concentrated salt solution and distilled water are injected on either side of the diaphragm. The solution in the two compartments, which is well stirred using glass stirrers, is sampled at predetermined time intervals. An Atomic Absorption Spectrophotometer is used for the analysis and withdraws small samples directly from each compartment. The temperature is also recorded during each experimental run. Results are reported in Appendix 7.6.

3.2.3. Geometry of the physical components of a diaphragm

The only type of diaphragm considered in this section is type 4. The thickness, B, of the diaphragm is determined by averaging a number of micrometer readings taken at various points along its surface. The void fraction is experimentally obtained by knowing the weight per unit area of the diaphragm and the density of the diaphragm material. Photomicrographs of a plan and sectional view of the diaphragm are taken and the magnification is calculated. Thread diameters, spacings and the number of warp and shute counts per unit length are measured. The photomicrographs are shown in Appendix 7.7 and the readings are recorded in Appendix 7.8.

3.3 Diffusion coefficients of Na^+, Cl^- and OH^- at elevated temperatures

The diffusion cell for this set of experiments is identical to the one described in

FIGURE 4

Apparatus for measuring pressure drop across Diaphragm

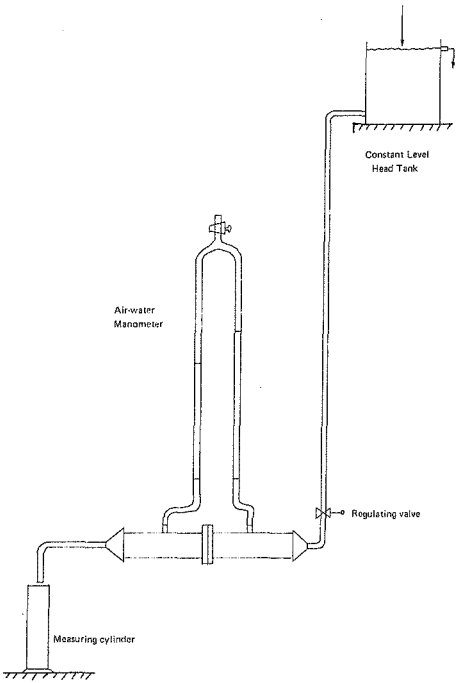
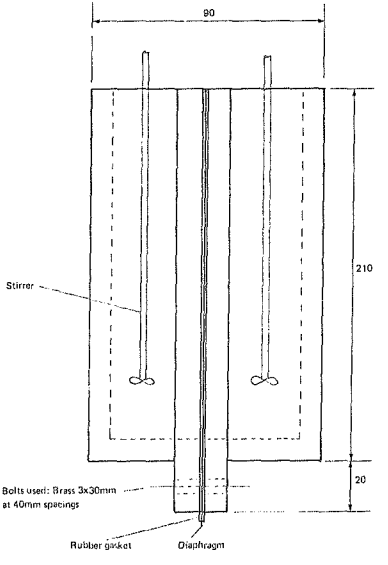


FIGURE 5

Apparatus for measuring the diffusion of an ion through a diaphragm
(All dimensions in mm.)



Internal Dimensions 70x100x190

Section 3.1.2, the only difference being its material of concentration, which is mild steel. The steel is used so that temperatures of up to 86°C can be achieved. The inside of the cell is painted with polyurethane to prevent corrosion of the steel at the high temperatures. The apparatus is set up as shown in figure 6. The whole cell is immersed in a constant temperature water-bath and preheated. The solutions to be used in the experiment are also preheated in the bath.

The solutions are made up to have approximately the same concentrations as those found in the anode and cathode compartments of the chlor-alkali cell. The concentrations used are: (i) Side 1: 4 molar NaCl and (ii) Side 2: 2,5 molar NaCl and 2,5 molar NaOH.

The experimental procedure is as follows. The cell and the two volumetric flasks containing the two solutions are heated up in the constant temperature water-bath. Once the solutions in the flasks are at the desired temperature, a known volume of each is poured into the cell on either side of the diaphragm. Glass stirrers are placed in each compartment to ensure good mixing. The two flasks are replaced in the water-bath with fresh solutions in them. After ten minutes the first 10ml samples are simultaneously withdrawn from both compartments. Equivalent amounts of the fresh solutions are returned to each compartment to maintain a constant volume. Using the same procedure, samples are withdrawn at predetermined time intervals up to 1½ hours. At the end of the experiment the volume of solution in the cell is measured.

The samples are then analysed for Na^+, Cl^- and OH^- (methods of analysis given in Appendix 7.9). The experimental readings are recorded in Appendix 7.10.

3.4 Results and discussion

3.4.1 Characterisation of diaphragm

The results of the pressure drop experiments can be found in figures 7, 8, 9 and 10. The graphs are plots of $\Delta p/u$ vs. u for the four different types of diaphragm. According to Armour and Cannon[15] (see Appendix 7.2) these plots should be straight lines with slope $\beta L \rho / \epsilon^2 D$ and intercept $\alpha \mu L(a/\epsilon)^2$. The experimental points fell reasonably well on straight lines, but for diaphragms 2 and 4 the slopes are negative. This means that the values of β will be negative. The values of α and β obtained by Armour and Cannon[14] were $\alpha = 8{,}61$ and $\beta = 0{,}52$. Measures of a, ϵ and D are known for diaphragm 4 and the corresponding values for α and β turned out to be $\alpha = 107$, $\beta = -0{,}52$.

Hence one can see that there does not appear to be any agreement between the experimentally determined behaviour of fluid flow through woven diaphragms and that predicted by Armour and Cannon. In the first instance the slopes of the plots for the two tighter woven diaphragms, i.e. diaphragms with a larger value for ϵ, are negative, and in the second the actual values of α and β obtained for diaphragm 4 are far different from those found by Armour and Cannon. The reasons for these discrepancies can be attributed to, (i) the fact that under increasing pressure difference the diaphragm stretches and bows. This causes the area as well as the mean pore size to increase, and (ii) the fact that the equations derived by Armour and Cannon were under the

FIGURE 6

Apparatus to measure Diffusion Coefficients at elevated temperatures

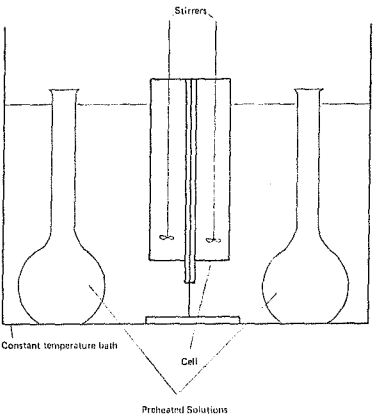


FIGURE 7

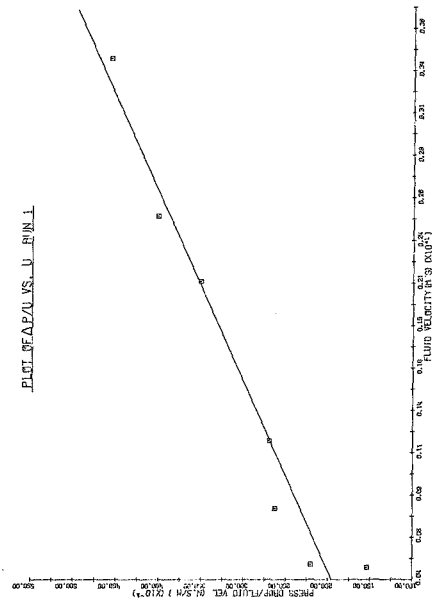

PLOT OF ΔP/L VS. U RUN 1
PRESS DROP/FLUID VEL GM/CM**2 SEC/CM (X10**3)
FLUID VELOCITY CM/SEC (X10**-1)
0.00
50.00
100.00
150.00
200.00
250.00
300.00
350.00
400.00
450.00
500.00
550.00
600.00
650.00
700.00
0.05
0.09
0.11
0.14
0.16
0.18
0.21
0.25
0.29
0.31
0.34
0.39

FIGURE 8

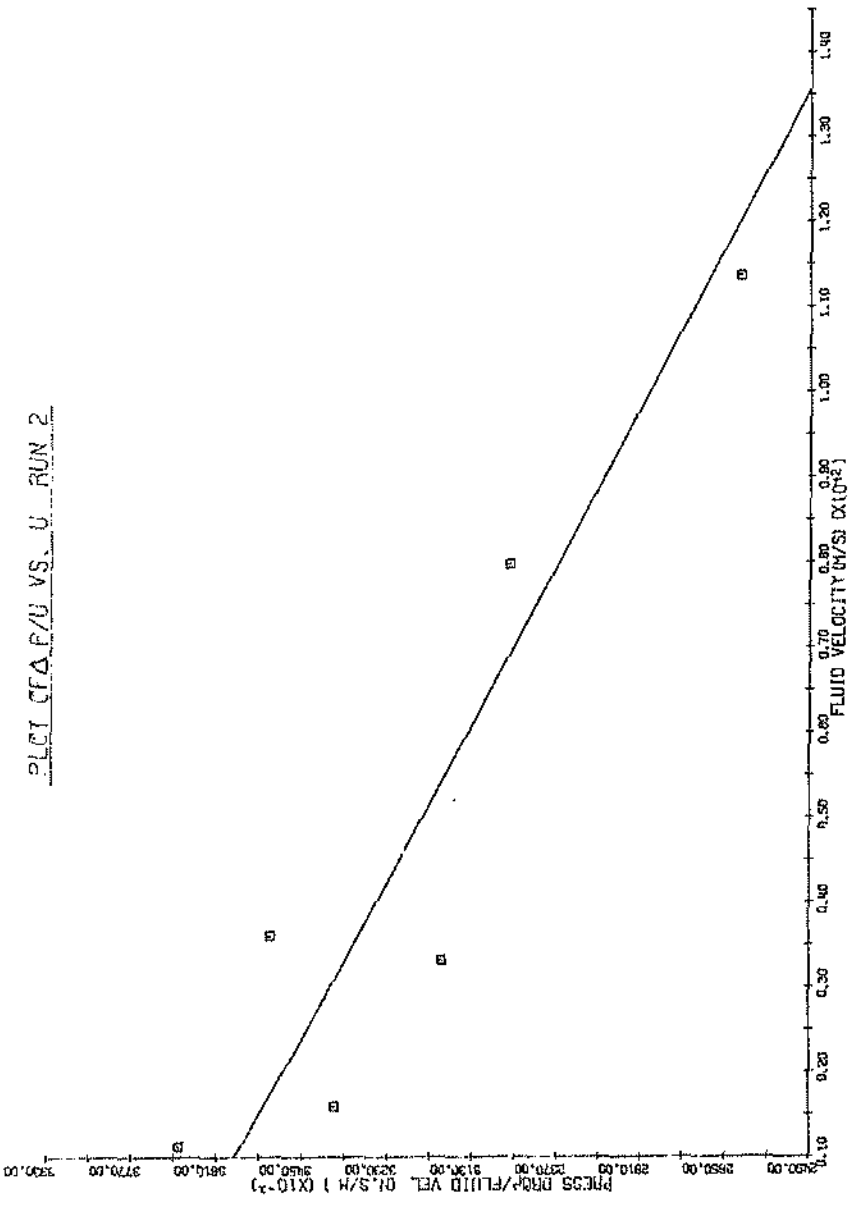


FIGURE 9

PLOT OF A.P/U VS. U RUN 3
PRESS DROP/FLUID VOL. (N.S/M) X10^5
FLUID VELOCITY(M/S) X10^1

FIGURE 10

PLOT OF ΔP/L VS. U RUN 4
PRESS DROP/FLUID VEL. (LB/FT³) (10⁻³)
FLUID VELOCITY (FPS) X10⁻²
100.00
180.00
260.00
340.00
420.00
0.10
0.30
0.50
0.70
0.90
1.10
1.30
1.50
1.70
1.90
2.10
2.30
2.50
2.70

assumption that the diaphragm threads were solid cylinders in point contact. For woven cloth diaphragms this assumption is likely to introduce error.

The results of the diffusion experiments are presented in figures 11, 12, 13, and 14. They show plots of $\ln \Delta c$ vs time for the four different diaphragms. The theory, from Appendix 7.3, predicts that the plots should be straight lines with slope $= -2DA/Vol$. The experimental points fall very close to straight lines for all the runs. The values of the diffusion coefficient of the sodium ion obtained are listed on Table 2.

TABLE 2

Diaphragm:	Diffusion Coefficient (cm^2/s):
1	$7,15 \times 10^{-5}$
2	$2,64 \times 10^{-5}$
3	$6,41 \times 10^{-5}$
4	$11,43 \times 10^{-5}$

It can be seen that the diffusion coefficient increases with increasing void fraction, which is to be expected as a high void fraction indicates a less tightly woven diaphragm with a larger pore diameter.

The physical properties of diaphragm 4 are calculated from measurement taken from the photomicrographs. The magnification of the photomicrographs is 17.5 times. Table 3 gives a comparison between measured values and those calculated from equations presented in Appendix 7.4.

TABLE 3

VALUE	MEASURED	CALCULATED	ERROR
Diaphragm thickness (m)	$1,374 \times 10^{-3}$	$1,420 \times 10^{-3}$	3
Warp diameter (m)	$5,710 \times 10^{-4}$		
Shute diameter (m)	$4,290 \times 10^{-4}$		
Distance between warp wires, l_{2s}, (m)	$7,79 \times 10^{-4}$	$\frac{1}{N_w} = 8,19 \times 10^{-4}$	5
Warp counts/m, N_w	1224		
Shute counts/m, N_s	1170		
Surface area/unit vol.,a, (m^{-1})		4300	
Void fraction, ϵ	0,67	0,50	25

The agreement between calculated and measured values of diaphragm thickness, B, and distance between warp wires, l_{2s}, is good (~4% error). There is however an error of 25% between the calculated and measured value of the void fraction, ϵ. The reason for this is that the measured value is calculated using the mass per unit area and the material density, while the calculated value is found from values measured off the photomicrographs. For the calculated value the following assumptions are made: (i) the threads

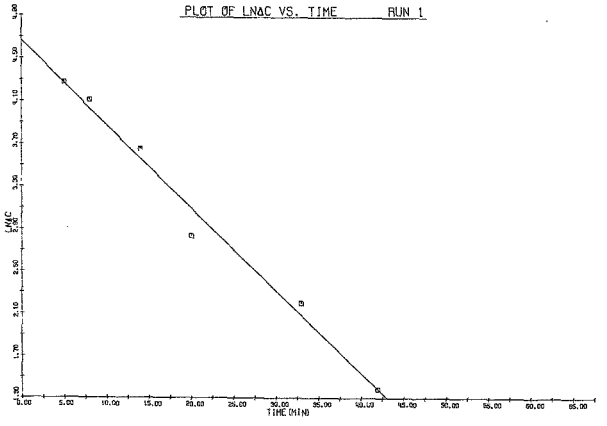

PLOT OF LNAC VS. TIME RUN 1
LNAC
TIME (MIN)
4.90
4.50
4.10
3.70
3.30
2.90
2.50
2.10
1.70
1.30
0.00
5.00
10.00
15.00
20.00
25.00
30.00
35.00
40.00
45.00
50.00
55.00
60.00
65.00

FIGURE 11

FIGURE 12

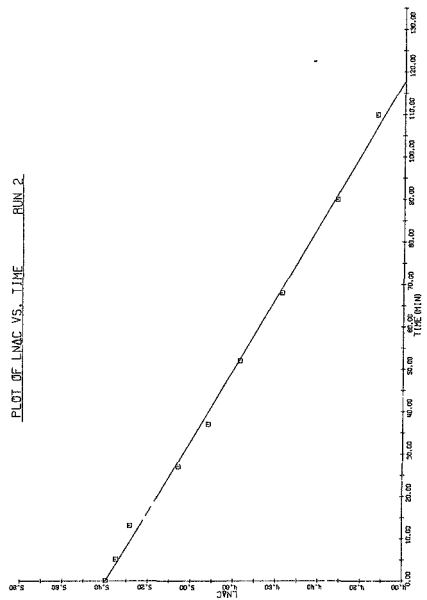

PLOT OF LNAC VS. TIME RUN 2
LNAC
TIME(MIN)
4.00
4.20
4.40
4.60
4.80
5.00
5.20
5.40
5.60
5.80
0.00
10.00
20.00
30.00
40.00
50.00
60.00
70.00
80.00
90.00
100.00
110.00
120.00
130.00

FIGURE 13

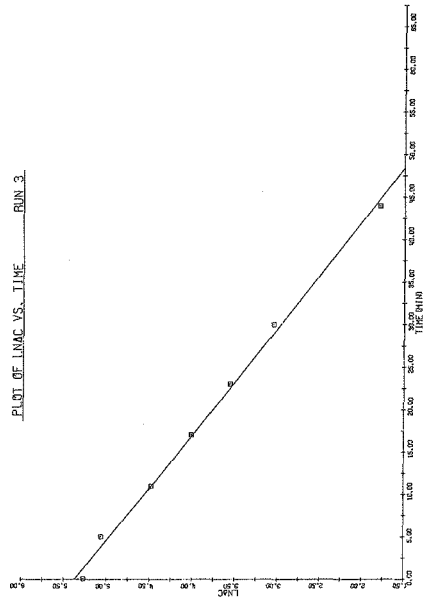
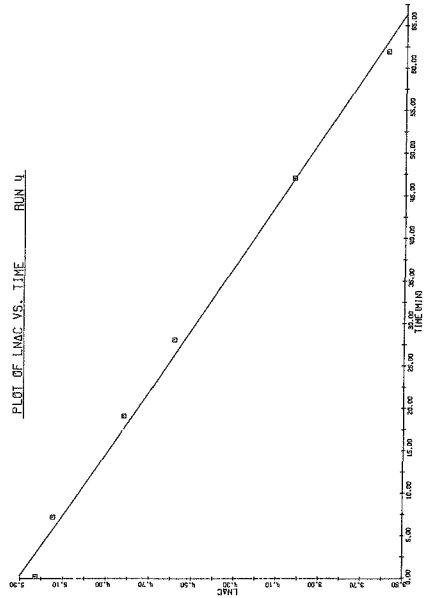

PLOT OF LNAC VS. TIME RUN 3
LNAC
TIME (MIN)
6.30
5.90
5.50
5.08
4.68
4.28
3.87
3.47
3.06
2.66
2.25
0.00
5.00
10.00
15.00
20.00
25.00
30.00
35.00
40.00
45.00
50.00
55.00
60.00
65.00

FIGURE 14


PLOT OF LNAC VS. TIME RUN 4
LNAC
TIME(MIN)
0.00
5.00
10.00
15.00
20.00
25.00
30.00
35.00
40.00
45.00
50.00
55.00
60.00
3.30
3.70
4.10
4.50
4.90
5.30
5.70
6.10
6.50

are solid cylinders and (ii) the threads make point contact. These assumptions are obviously not valid and probably account for the 25% deviation observed. The calculated value is lower because it does not take into account the porous nature of the threads in the diaphragm.

3.4.2. Diffusion coefficients at elevated temperatures

The results of this set of experiments can be found in figure 15. This is a plot of the diffusion coefficients of the sodium, chloride and hydroxyl ions as a function of temperature. The basic trend is for the diffusion coefficients to increase with increasing temperature. The coefficients of Na^+, Cl^- and OH^- are approximately equal to 1.5×10^{-5} cm^2/s at 25° C, while at 85° C the value is about 10.5×10^{-5} cm^2/s. The curves for Na^+, Cl^- and OH^- intersect at a temperature of 82° C, below this temperature the order of magnitude of the diffusion coefficients is $Na > OH^- > Cl^-$, while above it the order is $Cl^- > OH^- > Na^+$.

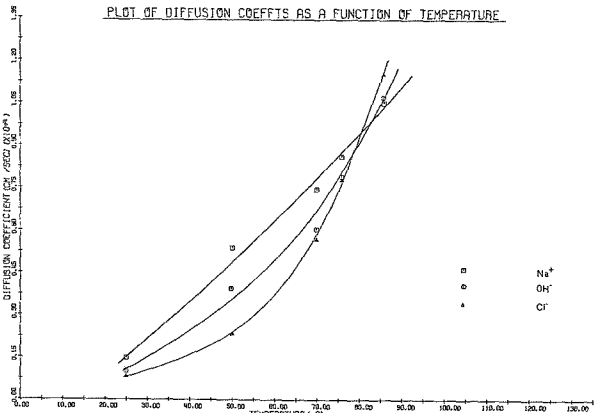

PLOT OF DIFFUSION COEFFTS AS A FUNCTION OF TEMPERATURE
DIFFUSION COEFFICIENT (CM /SEC) X(10**)
TEMPERATURE (C)
0.00
10.00
20.00
30.00
40.00
50.00
60.00
70.00
80.00
90.00
100.00
110.00
120.00
130.00
Na+
OH-
Cl-

FIGURE 15

4. EXPERIMENTS ON CHLOR-ALKALI CELL

4.1 *Details of apparatus*

The chlor-alkali cell consists of three sections: (i) the anode compartment, (ii) the cathode compartment, and (iii) the cathode compartment lid. These are all bolted together as shown in figure 16. The material of construction of the cell is glass-fibre reinforced resin.

The brine solution inlet and chlorine outlet are built into the anode compartment, which is fitted with a slot in its roof to house the anode. The anode is of the flow-through type made from titanium with a ruthenium oxide coating. The current is fed to the anode via a copper busbar bolted to it. The anolyte solution level is indicated on a glass tube inserted near the base.

The cathode is 16 mesh expanded mild steel and is attached to the cathode compartment lid. Current is fed to it via a copper busbar. A hole is provided in the lid to allow for temperature measurements and for sampling.

The solution flows into the anode compartment, passing through the anode and into the cathode compartment. Here it passes through the cathode and flows to the outlet of the cell which is located in the lower half of this compartment. The catholyte level is also indicated on a glass tube inserted in the base of the compartment.

The cell is assembled by stretching the diaphragm between the anode and cathode compartments and bolting them together. The cell is sealed with rubber gaskets. The cathode lid and gasket are then bolted into position with the cathode fitting into the slots provided in the cathode compartment.

Figure 17 shows the experimental layout. The concentrated brine solution is fed from a feed tank, through a copper coil immersed in a constant temperature water bath, via a rotameter, to the anode compartment of the cell. The water bath and copper coil preheat the solution to the desired inlet temperature. After passing through the cell, the solution flows into an overflow tank. A power supply with operating ranges 0–100A and 0–25 volts, is connected as shown. The cell is housed in a fume chamber to extract the chlorine gas evolved.

4.2 Experimental procedure

The constant temperature bath is switched on and allowed to reach its set temperature of 60°C. The valves are opened and the system is filled with salt solution. Once the flow has reached steady state, the mass of the feed tank and the time are noted and the power supply is switched on. The power supply has to be regulated during the transient period until the desired current is obtained. The system is allowed to run at constant flow rate and current density for about 2 to 2½ cell residence times.

After this time has elapsed the cell temperature is taken and the anolyte and catholyte

FIGURE 16

Chlor-alkali experimental cell
(All dimensions in mm)

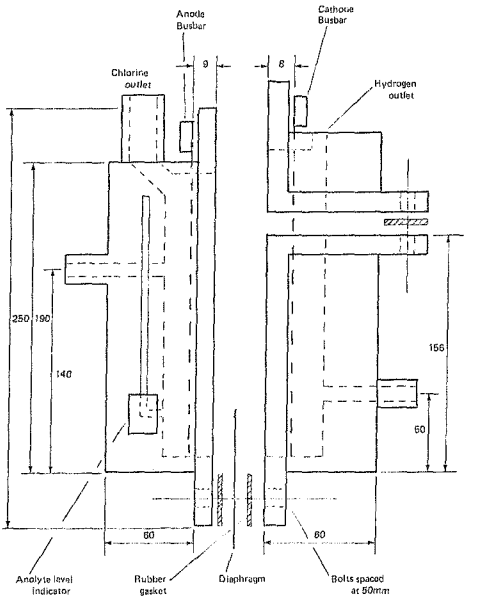
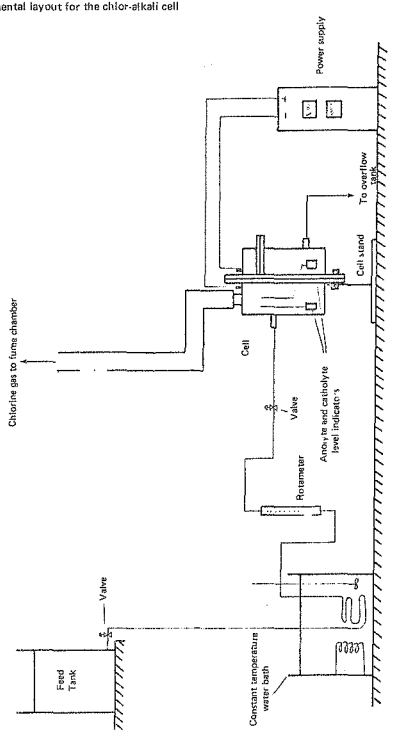


FIGURE 17

Experimental layout for the chlor-alkali cell



are sampled. The valves are closed and the mass of the feed tank and the time are noted. A sample is also withdrawn from the feed tank. The power supply and the water bath are then switched off.

The samples are then analysed for sodium, chloride, hydroxide (or pH), chlorate and hypochlorite ion concentration. The analytical methods used for the first three ions are presented in Appendix 7.9 and the results are recorded in Appendix 7.12.

5. RESULTS, DISCUSSION AND CONCLUSION

A mass balance is performed over the cell for each run according to the logic diagram given in Appendix 7.12. The parameters calculated in this mass balance are anodic efficiency, ion fluxes, water lost over anolyte and catholyte, flow rate through diaphragm and outlet flow rate. A check for this mass balance is the value of the outlet flow rate. This flow rate is calculated in two different ways: (i) from an overall Na^+ balance, and (ii) from the overall mass balance. For each run these two values agreed to within 5% of each other.

Values of parameters predicted by the model are compared to those found by experiment in Appendix 7.13. Table 4 lists these parameters for a typical run.

TABLE 4

Run 11: current = 55A, voltage = 4,5V., diaphragm area = 265cm^2, mass flow rate in = 0,342g/s

VARIABLE	EXPERIMENTAL	MODEL	%ERROR
Temperature	73,0	72,5	1
ζ	0,890	0,910	2
N_3	$-0{,}124\times10^{-6}$	$-0{,}122\times10^{-6}$	8
pH	5,1	5,2	2
A_1	4,39	4,34	1
A_2	4,30	4,34	1
A_4	0,03	0,027	10
C_1	5,24	5,34	2
C_2	3,49	3,53	1,5
C_3	1,78	1,82	2
Q_d	0,287	0,286	0
Q_o	0,265	0,270	2

The agreement between values predicted by the model and those found by experiment is good. The error is in most cases less than 5% which is well within experimental accuracy.

The remainder of the runs followed a similar pattern with the model providing a good fit to experimentally determined values. The one exception to this is Run 1. Here, the inlet flow rate is very low and this results in a large OH^- back migration value and a low anodic efficiency. In this case the model predicts anolyte and catholyte concentrations which differ by 20% and 50% respectively from the experimental values.

A summary of the variables, the range over which they are tested, and the error between predicted and experimental values is given in Table 5.

TABLE 6

VARIABLE	RANGE	% ERROR LESS THAN:
Anolyte (Na^+)	3,6 – 5,1 molar	4
Anolyte (Cl^-)	3,6 – 5,1 molar	4
Anolyte (ClO^-)	0,002 – 0,07 molar	13
Catholyte (Na^+)	4,9 – 5,9 molar	3,5
Catholyte (Cl^-)	1,05 – 3,3 molar	6,5
Catholyte (OH^-)	2,5 – 4,0 molar	7
Anolyte pH	3 – 5,3	28
Outlet flow rate	0,165 – 0,735 cm^3/s	4
Cell temperature	60 – 89°C	2
Efficiency	0,78 – 1,0	1,5

The only large error in a variable predicted by the model arises in the anolyte pH. This can be explained by looking at the equations used to calculate it. These are equations 2.36 and 2.37 in section 2.6. The second equation is based on the assumption that all the anodic inefficiency goes to the evolution of oxygen. This is a reasonable assumption as shown by the small amounts of chlorate and hypochlorite that are formed. The first equation is an empirical one given by Nagy[9] and is based on data from an experimental cell. Nagy admits that this equation is scale dependent and therefore changes with different cell design. This equation is used nevertheless to complete the model.

Other assumptions which are used in formulating the model, and which could lead to errors, are: (i) anolyte and catholyte are well mixed, (ii) transport of ions in the diaphragm obeys the dilute solution form of the flux equation, (iii) negligible amounts of chlorate and hypochlorite are produced, and (iv) anolyte and catholyte temperatures are approximately equal.

Assumption (i) should not introduce a large error as gas bubbling would be expected to agitate the solution sufficiently. The use of the dilute solution flux equation has been discussed in section 2.2 and it is possible that it could introduce an error of approximately 10 in the calculation of the fluxes. Assumption (iii) does not affect the mass balance to any great extent, but it can affect the predicted anodic efficiency. This is because the model, as it stands, assumes that the inefficiency is due to oxygen evolution alone. A more detailed version of the model should include electrolytic chlorate formation as an inefficiency reaction.

In fullscale chlorine-caustic production cells there is a temperature difference of a few degrees centigrade between anolyte and catholyte[3]. The model, according to assumption (iv), uses the same value for anolyte and catholyte temperature, but this introduces an error of less than 5% in the energy balance.

The proposed model uses two equations that have adjustable parameters which are fitted using experimentally determined data. They are the equations used for calculating the anolyte pH and the OH^- transport numbers. The first has already been discussed and the

latter can be correlated with the catholyte OH^- concentration.

It can be seen from the results in Table 5 that the mechanistic type model proposed, with its simplifying assumptions, simulates to a reasonable degree the experiments performed on a laboratory scale chlor-alkali cell.

The geometric properties of the diaphragm such as void fraction and mean pore diameter do not appear in the model. This is because the diffusion coefficients used in the model were found experimentally with a diaphragm identical to that used in the chlor-alkali cell.

The results presented in this thesis indicate that future work on the modelling of this type of cell should be directed to studying: (i) the effect of diaphragm material and geometry on ionic diffusion coefficients, (ii) the effect of ionic interactions on the transport of OH^- in the diaphragm, and (iii) the kinetics of electrode processes at the anode and how they are affected by anolyte composition, temperature and current density.

6. REFERENCES

1. Bianchi, G: 'Fundamental and Applied Aspects of the Electrochemistry of Chlorine'. *Journal of Applied Electrochemistry*, 1:231-243, (1971).

2. Staff writers: 'Technical Developments for Diaphragm-Processes, Electrolytic Facilities and Process Conversion Plan'. *Chemical Economy and Engineering Review*, 5 No. 8:45-48 (1973).

3. MacMullin, R.B.: 'Computer Simulation of a Diaphragm Cell for Chlor-Alkali Production'. *Denki Kagaku*, 38 No. 8:570-579, (1970).

4. Solray et Cie.: 'Diaphragm for an Electrolysis Cell'. *Belg. 814510* (Cl. Bo1k), 02 Sept. 1974, Appl. 800949, 15 Jun. 1973

5. Faita, G. & Fiori, G.: 'Anodic Discharge of Chloride Ions on Oxide Electrodes'. *Journal of Applied Electrochemistry*, 2:31-35, (1972).

6. Hammer, L. & Wranglén, G.: 'Cathodic and Anodic Efficiency Losses in Chlorate Electrolysis'. *Electrochimica Acta*, 9:1-16, (1964).

7. Hine, F. & Yasuda, M.: 'On the Cathode Reaction in Solutions Containing ClO_3^-'. *J. Electrochem. Soc.*, 118 No. 1:182-183, (1971).

8. De Valera, V.: 'On the Theory of Electrochemical Chlorate Formation'. *Trans Faraday Soc.*, 49:1338, (1953).

9. Nagy, Z.: 'A Mechanistic Model for the Calculation of Material Balance for a Diaphragm-type Chlorine Caustic Cell'. *J. Electrochem. Soc.*, 124 No. 1:91-95, (1977).

10. Cerquetti, A., Longhi, P., Mussini, T. and Natta, G.: *J. Electroanal. Chem.*, 20: 411, (1969).

11. Newman, J.S.: *Electrochemical Systems*. Englewood Cliffs, N.J.: Prentice-Hall, Inc., 1973.

12. MacMullin, R.B.: 'Algorithms for the Vapor Pressure of Water over Aqueous Solutions of Salt and Caustic Soda'. *J. Electrochem. Soc.*, 116 No. 3:416-419, (1969).

13. Mussini, T. & Pagella, A.: 'Activity Coefficients and Transference Numbers of Aqueous NaCl and $CaCl^2$ at Various Temperatures and Concentrations'. *La Chimica e L'Industria*, 52 No. 12:1187-1191, (1970).

14. Weast, R.C.: *Handbook of Chemistry of Physics*. 56th Ed. Cleveland, Ohio: CRC Press, 1975-6.

15. Armour, J.C. & Cannon, J.N.: 'Fluid Flow Through Woven Screens'. *AIChE. Journal*, 14 No. 3:415-420, (1968).

7. APPENDIX

7.1 Types of Diaphragms used

PROPERTY	TYPE 1	TYPE 2	TYPE 3	TYPE 4
mass/unit area (g/m^2)	125,5	170,0	284,8	415,0
Air permeability $m^3 air/m^2/min.$ @ 13mm W.G.	2,5	4,5 – 6,0	5,0	1,5 – 3,0
Weave	1x1 plain	2x1 plain Dutch	3x1 Crowfoot	2x2 twilled Dutch
Material	Nylon	Polypropylene	Terylene	Polypropylene
Thickness, B (m)	$3,15x10^{-4}$	$7,5x10^{-4}$	$2,7x10^{-4}$	$1,374x10^{-3}$
void fraction ϵ^*	0,65	0,55	0,58	0,67

* $\epsilon = \left(1 - \frac{\text{mass/area} \times 10^{-6}}{\rho B}\right)$

ρ Polypropylene = 0,91 g/cm^3

ρ Nylon = 1,14 g/cm^3

ρ Terylene = 1,38 g/cm^3

7.2 Theory for pressure drop experiments

The equation derived by Armour and Cannon[14] is:

$$f = \frac{\alpha}{N_{RE}} + \beta \qquad 7.1$$

where f is the screen friction factor and is given by:

$$f = \frac{\Delta p \epsilon^2 D}{L \rho u^2} \qquad 7.2$$

and N_{RE} is the screen Reynolds number given by:

$$N_{RE} = \frac{\rho u}{\mu a^2 D} \qquad 7.3$$

Substituting 7.2 and 7.3 in 7.1 and rearranging:

$$\frac{\Delta p}{u} = \alpha \frac{\mu L}{\epsilon^2 D} a^2 + \frac{\beta L \rho}{\epsilon^2 D} u \qquad 7.4$$

Hence a plot of $\Delta p/u$ vs. u should yield a straight line with slope $\frac{\beta L \rho}{\epsilon^2 D}$ and intercept $\alpha \mu L (\frac{a}{\epsilon})^2$

7.3 Theory for diffusion of an ion across a diaphragm

From section 2.2 the flux equation in one direction can be written as:

$$N_i = -u_i c_i Z_i F \frac{dE}{dx} - D_i \frac{dc_i}{dx} + c_i v \qquad 7.5$$

Equation 7.5 reduces to the following equation under the conditions of: (i) no flow, (ii) no potential difference, (iii) the assumption that any potential gradient caused by concentration differences is negligible.

$$N_i = -\frac{D_i dc_i}{dx} \qquad 7.6$$

In the diaphragm the following assumptions are made: (i) a linear concentration profile exists, (ii) pseudo steady-state exists, i.e. the flux of an ion is constant throughout the diaphragm. Hence the concentration gradient $\frac{dc}{dx}$ can be expressed as:

$$\frac{dc}{dx} = \frac{(c_i)_2 - (c_i)_1}{l} \qquad 7.7$$

Where subscripts 1 and 2 denote the compartments on either side of the diaphragm and l is the diaphragm thickness.

A mass balance over the two compartments of the experimental cell yields:

Compartment 1: $$\frac{d(c_i Vo)_1}{d\tau} = \frac{-N_i A D_i \{(c_i)_2 - (c_i)_1\}}{l} \qquad 7.8$$

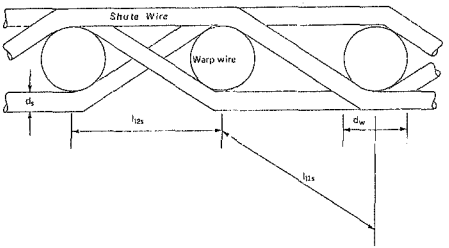
Compartment 2: $$\frac{d(c_i Vo)_2}{d\tau} = \frac{N_i A D_i \{(c_i)_2 - (c_i)_1\}}{l} \qquad 7.9$$

Assuming that the volume of each compartment, Vo, remains constant, combining equations 7.8 and 7.9, and integrating, the following expression is obtained:

$$\ln\{(c_i)_2 - (c_i)_1\} = -\frac{2D_i A}{Vo.l} \cdot \tau \qquad 7.10$$

Hence a plot of $\ln\Delta c$ vs. time (τ) should yield a straight line with slope $\frac{-2D_i A}{Vo.l}$

7.4 Equations for calculating diaphragm geometric properties



Diaphragm type no. 4 – twilled dutch weave.

Diaphragm thickness, B,

$$B = d_w + 2d_s \qquad 7.11$$

Surface area to unit volume ratio, a,

unit volume = 1 x 1 x B

area of warp wires in unit volume = $\pi d_w . N_w$

area of shute wires in unit volume = $\frac{\pi N_s d_s N_w}{2} (l_{11s} + l_{12s})$

hence: $a = (N_w d_w + \frac{N_s d_s}{2} + \frac{N_s N_w d_s l_{11s}}{2})$ 7.12

Distance between warp wires, l_{12s},

$$l_{11s} = \sqrt{(d_w + d_s)^2 + l_{12s}^2} \qquad 7.13$$

Void fraction, ϵ

unit volume = 1 x 1 x B

volume of warp wires in unit volume = $\frac{\pi d_w^2 N_s}{4}$

volume of shute wires in unit volume = $\frac{\pi d_s^2 N_s}{4}\left(\frac{1}{\sin\theta} + \frac{N_w}{2} l_{11s}\right)$

hence: $\epsilon = 1 - \frac{\pi}{4B}\{N_w d_w^2 + \frac{1}{2} N_s d_s^2 + \frac{1}{4} N_s N_w d_s^2 l_{11s}\}$ 7.14

7.5 Readings from pressure drop experiments

DIAPHRAGM	PRESSURE DROP (cmH_2O)	FLOW RATE (ml/min.)
Type 1	16,2	625,3
	10,4	456,0
	7,73	386,7
	3,63	218,7
	2,20	147,0
	1,30	88,0
	0,90	84,7
Type 2	30,5	209,0
	25,1	144,5
	15,6	65,3
	10,9	60,7
	5,6	29,1
	4,2	20,1
Type 3	21,0	650,1
	16,8	622,1
	12,9	495,9
	8,5	274,3
	4,2	181,7
	1,2	60,1
Type 4	36,3	404,5
	35,5	400,1
	33,0	390,3
	32,9	320,7
	29,7	224,1
	21,7	126,3
	11,4	54,7
	5,5	245,0

Plots of $\Delta p/u$ vs. u for these experimental runs are given on figures 7 – 10.

7.6 Readings from diffusion experiments

Run 1

Diaphragm type 1, temperature = 17,5°C, diaphragm area = 167cm², total volume of solution = 1160cm³

c_1 (ppm)	c_2 (ppm)	TIME (min)	Δc(ppm)	$\ln\Delta c$
92	20	5	72	4,277
87	26	8	61	4,111
73,5	35	14	38,5	3,651
62,5	45,5	20	17	2,833
59	50	33	9	2,197
57	53	42	4	1,386

Run 2

Diaphragm type 2, temperature = 18°C, diaphragm area = 157cm², total volume of solution = 1080cm³

c_1 (ppm)	c_2 (ppm)	TIME (min)	Δc (ppm)	$\ln\Delta c$
220	0	0	220	5,394
220	10	5	210	5,347
215	18	13	197	5,283
190	33	27	157	5,056
183	46	37	137	4,920
173	55	52	118	4,771
162	65	68	97	4,575
154	79	90	75	4,317
146	84	110	62	4,127

Run 3

Diaphragm type 3, temperature = 19°C, *diaphragm* area = 156cm², total volume of solution = 1080cm³

c_1 (ppm)	c_2 (ppm)	TIME (min)	Δc(ppm)	$\ln\Delta c$
210	16	0	194	5,268
190	33	5	157	5,056
155	67	11	88	4,477
138	83	17	55	4,007
129	94	23	35	3,555
121	100	30	21	3,045
114	108	44	6	1,792

Run 4

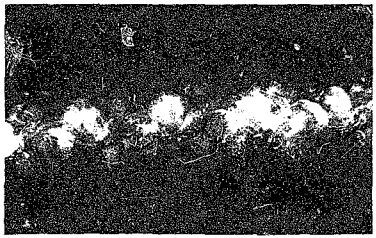
Diaphragm type 4, temperature = 17,5°C, diaphragm area = 154cm², total volume of solution = 1080cm³

c_1 (ppm)	c_2 (ppm)	TIME (min)	Δc(ppm)	$\ln\Delta c$
186	0	0	186	5,226
185	13	7	172	5,147
160	36	19	124	4,820
146	48	28	98	4,585
126	70	47	56	4,025
116	80	62	36	3,584

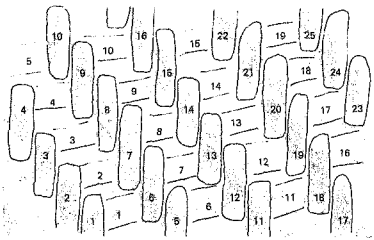
Plots of $\ln\Delta c$ vs. time for these experimental runs are given on figures 11 – 14.

7.7 Photomicrographs of diaphragm type 4

MAGNIFICATION 17.5 TIMES



CROSS SECTIONAL VIEW : SHOWING ENDS OF WARP THREADS



PLAN VIEW : WARP THREADS RUNNING HORIZONTALLY

7.8 Measurements of the physical components of a diaphragm

Diaphragm thickness, B (cm) :

	0,1401
	0,1351
	0,1370
Average	0,1374

Warp wires/unit length, N_w (counts/m):

LENGTH (m)	NO. OF COUNTS	N_w
0,1016	123	1210,6
0,0762	93	1220,5
0,0508	63	1240,2
	Average	1224

Shute wires/unit length, N_s (counts/m):

LENGTH (m)	NO. OF COUNTS	N_s
0,1016	219	2155,5
0,0508	111	2185,0
	Average	2170

Distance between warp wires (edge to edge) (from photomicrograph):

WIRE NOS.	DISTANCE (cm)
7 & 8	2,30
13 & 14	2,45
6 & 7	2,42
9 & 10	2,30
1 & 2	2,35
Average	2,36

Diameter of warp wires: d_w, (from photomicrograph)

WIRE NO.	DIAMETER (cm)	WIRE NO.	DIAMETER (cm)
1	1,00	11	1,10
2	1,05	12	0,98
3	1,08	13	1,00
4	0,98	14	1,00
5	1,10	15	0,95
6	0,90	16	0,95
7	0,95	17	1,00
8	0,95	18	0,98
9	1,10	19	0,98
10	1,00	Average	1,00

Diameter of shute wires: d_s, (from photomicrograph)

WIRE NO.	DIAMETER (cm)	WIRE NO.	DIAMETER (cm)
1	0,88	13	0,75
2	0,80	14	0,72
3	0,75	15	0,77
4	0,80	16	0,73
5	0,85	17	0,70
6	0,80	18	0,72
7	0,78	19	0,70
8	0,73	20	0,80
9	0,85	21	0,78
10	0,73	22	0,76
11	0,90	23	0,76
12	0,75	24	0,75
		Average	0,75

7.9 Methods of analysis for Na^+ Cl^- and OH^-

(i) Sodium ion:

The analysis of the Na^+ ion is performed using an Atomic Absorption Spectrophotometer. The wavelength used is 330,1 nm, and the concentration range is 100 to 300 ppm. The samples taken from the chlor-alkali cell and the elevated temperature diffusion cell are first diluted down into the above range.

(ii) Hydroxyl ion:

The anlysis of the OH^- ion is performed by titration with sulphuric acid. Phenolphthalein is used as the indicator.

(iii) Chloride ion:

The Cl^- ion is analysed by titration with silver chloride. The sample is diluted with 50ml distilled water, acidified with a few drops of 6N. HNO_3 and then neutralised with $CaCO_3$. The indicator is potassium dichromate.

7.10 Readings of diffusion experiments at elevated temperatures
(All concentrations in this sub-section in g/l.)

Run 1:
Temperature 25°C, diaphragm area = 90,5cm², total volume = 625cm³

TIME (min)	SIDE 1			SIDE 2		
	Na^+	OH^-	Cl^-	Na^+	OH^-	Cl^-
0	87,6	0,0	135,0	108,4	39,2	85,1
20	88,0	0,7	134,0	106,8	38,5	84,4
50	89,3	2,3	132,6	106,0	36,9	86,5
80	90,3	3,1	132,6	106,0	36,1	86,5
125	90,6	5,6	128,0	104,4	33,6	90,8
160	92,0	6,2	128,7	103,5	33,0	90,8

Run 2:
Temperature 50°C, diaphragm area = 103cm², total volume = 740cm³

TIME (min)	SIDE 1			SIDE 2		
	Na^+	OH^-	Cl^-	Na^+	OH^-	Cl^-
0	87,8	2,6	130,1	108,5	39,4	85,1
15	90,9	10,0	119,1	104,5	32,0	93,9
36	93,5	13,4	116,3	103,0	26,6	99,3
57	95,3	14,3	116,9	102,5	27,7	100,3
93	97,5	15,8	116,9	101,2	26,1	102,0

Run 3:
Temperature 70°C, diaphragm area = 103cm², total volume = 740cm³

TIME (min)	SIDE 1			SIDE 2		
	Na^+	OH^-	Cl^-	Na^+	OH^-	Cl^-
0	87,8	2,6	130,1	108,5	39,4	85,1
11	89,6	10,0	117,3	104,9	32,0	95,0
34	93,0	13,8	114,5	103,5	28,3	100,7
60	95,1	15,5	114,1	101,7	26,5	101,4
90	96,2	17,9	114,0	100,0	24,1	104,2

Run 4:
Temperature 76°C, diaphragm area = 151cm², total volume = 920cm³

TIME (min)	SIDE 1			SIDE 2		
	Na^+	OH^-	Cl^-	Na^+	OH^-	Cl^-
10	91,8	10,8	119,0	104,5	30,8	97,1
31	93,1	14,5	113,5	100,0	27,1	98,2
61	95,2	17,7	110,0	100,5	23,9	105,0
95	97,6	19,8	109,1	99,1	21,8	107,3

Run 5:
Temperature 86°C, diaphragm area = 145cm², total volume = 910cm³

TIME (min)	SIDE 1			SIDE 2		
	Na^+	OH^-	Cl^-	Na^+	OH^-	Cl^-
11	93,1	12,0	118,0	105,0	30,1	99,3
37	96,2	17,1	112,4	102,3	25,0	104,5
65	97,1	19,3	109,2	99,2	22,7	104,9
95	97,3	21,2	106,6	98,1	22,0	105,0

Plots of ln c vs. time are drawn for each of the three ions for every run. The slopes of these plots give the values of the diffusion coefficients. A summary of the diffusion coefficients as a function of temperature is given below :

TEMPERATURE	DIFFUSION COEFFICIENTx10^5 (cm^2/s)		
	Na^+	OH^-	Cl^-
25	1,48	1,01	0,81
50	5,39	3,95	2,33
70	7,46	6,05	5,69
76	8,61	7,91	7,79
86	10,50	10,70	11,5

A plot of the above table is given on figure 15.

7.11 Readings from runs performed on the chlor-alkali cell

Sample 1	from head tank
Sample 2	from anode compartment
Sample 3	from cathode compartment

Run 1:
Current = 65A, voltage = 4,6v, temperature = 88,5°C, diaphragm area = 256cm^2, mass flow rate in = 0,120g/s

SAMPLE	pH	Na^+	Cl^-	OH^-	ClO_3^-	ClO^-
1	8,0	4,82	4,80			
2	5,0	3,73	3,38		0,03	0,03
3	11,3	6,50	2,38	3,98	0,01	

Run 2:
Current = 65A, voltage = 4,8v, temperature = 84°C, diaphragm area = 260cm^2, mass flow rate in = 0,323g/s

SAMPLE	pH	Na^+	Cl^-	OH^-	ClO_3^-	ClO^-
1	6,0	4,72	4,71			
2	4,9	3,99	3,90		0,05	0,059
3	11,4	5,20	3,11	2,06	0,03	

Run 3:
Current = 65A, voltage = 4,8v, temperature = 83°C, diaphragm area = 250cm^2, mass flow rate in = 0,322g/s

SAMPLE	pH	Na^+	Cl^-	OH^-	ClO_3^-	ClO^-
1	6,4	4,92	4,90			
2	4,6	3,64	3,56		0,05	0,002
3	11,3	5,28	2,43	2,78	0,03	

* (All concentrations in this sub-section in moles/litre)

Run 4:
Current = 65A, voltage = 4,8v, temperature = 87°C, diaphragm area = 250cm², mass flow rate in = 0,235g/s

SAMPLE	pH	Na^+	Cl^-	OH^-	ClO_3^-	ClO^-
1	7,5	4,74	4,74			
2	4,8	3,88	3,74		0,08	0,01
3	11,7	5,70	2,49	3,10	0,03	

Run 5:
Current = 65A, voltage = 5,0v, temperature = 77°C, diaphragm area = 260cm², mass flow rate in = 0,543g/s

SAMPLE	pH	Na^+	Cl^-	OH^-	ClO_3^-	ClO^-
1	*6,4*	*4,62*	*4,66*			
2	5,0	4,00	3,99		0,002	0,0055
3	12,0	5,00	3,24	1,68	0,002	

Run 6:
Current = 65A, voltage = 5,2v, temperature = 75°C, diaphragm area = 240cm², mass flow rate in = 0,687g/s

SAMPLE	pH	Na^+	Cl^-	OH^-	ClO_3^-	ClO^-
1	7,3	4,73	4,75			
2	5,0	4,31	4,25		0,002	0,013
3	12,1	4,94	3,74	1,12	0,002	

Run 7:
Current = 65A, voltage = 5,0v, temperature = 69°C, diaphragm area = 240cm², mass flow rate in = 0,882g/s

SAMPLE	pH	Na^+	Cl^-	OH^-	ClO_3^-	ClO^-
1	6,8	4,83	4,89			
2	3,0	4,48	4,45		0,002	0,005
3	11,9	5,05	3,95	1,05	0,001	

Run 8:
Current = 65A, voltage = 4,8v, temperature = 81°C, diaphragm area = 265cm², mass flow rate in = 0,472g/s

SAMPLE	pH	Na^+	Cl^-	OH^-	ClO_3^-	ClO^-
1	7,0	4,75	4,81			
2	5,0	4,08	4,01		0,04	0,002
3	12,0	5,19	3,34	1,78	0,03	

Run 9:
Current = 40A, voltage = 4,1v, temperature = 60°C, diaphragm area = 265cm², mass flow rate in = 0,288g/s

SAMPLE	pH	Na^+	Cl^-	OH^-	ClO_3^-	ClO^-
1	6,9	5,04	5,06			
2	5,0	4,30	4,28		0,002	0,02
3	11,9	5,27	3,44	1,81	0,002	

Run 10:
Current = 75A, voltage = 5,0v, temperature = 88°C, diaphragm area = 265cm², mass flow rate in = 0,297g/s

SAMPLE	pH	Na^+	Cl^-	OH^-	ClO_3^-	ClO^-
1	7,1	5,10	5,12			
2	4,9	4,07	4,00		0,02	0,03
3	12,2	5,99	2,60	3,30		

Run 11:
Current = 55A, voltage = 4,5v, temperature = 73°C, diaphragm area = 265cm², mass flow rate in = 0,342g/s

SAMPLE	pH	Na^+	Cl^-	OH^-	ClO_3^-	ClO^-
1	7,1	5,17	5,17			
2	5,1	4,39	4,30		0,003	0,03
3	12,1	5,24	3,49	1,78	0,002	

Run 12:
Current = 70A, voltage = 5,0v, temperature = 83°C, diaphragm area = 265cm², mass flow rate in = 0,335g/s

SAMPLE	pH	Na^+	Cl^-	OH^-	ClO_3^-	ClO^-
1	7,3	5,02	5,02			
2	4,9	3,91	3,87		0,02	0,0089
3	11,8	5,71	3,16	2,53	0,015	

7.12 Chlor-alkali cell – logic diagram of mass balance

The experimental readings given in Appendix 7.11 are processed using the following calculation scheme. Input variables are: (i) mass flow rate in, (ii) feed, anolyte and catholyte concentrations, (iii) geometry of cell, (iv) cell current, (v) voltage, and (vi) cell operating temperature.

Input data
Calculate densities using algorithm
Calculate volume flow rate in
Calculate volume flow rate out from overall Na^+ balance
Calculate Na^+ flux
Calculate anodic efficiency
Calculate OH^- and Cl^- fluxes
Calculate Cl_2, O_2, and H_2 production rates
Calculate vapor pressure of water over anolyte and catholyte
Calculate water lost over anolyte and catholyte
Calculate overall mass balances
Calculate volume flow rate out from mass balance
Perform energy balance to calculate heat lost from cell
Calculate overall heat transfer coefficient
Write results

A check for the mass balance is the volumetric outlet flow rate. This value is calculated in two different ways: (i) from an overall Na^+ balance, and (ii) from the overall mass balance. For every run, these two values agreed to within 5% of each other.

The relationship between the mass flow rate and the temperature of the feed solution at the inlet is:

$$t_1 = 13{,}384\ M_f + 33{,}7$$

The value of U, the overall heat transfer coefficient, obtained from the experiments is:

$$U = 1{,}270\ W/m^2{}^\circ C$$

7.13 Comparison of experimental results and those predicted by the model for the chlor-alkali cell

	RUN 1		RUN 2	
	EXPERIMENTAL	MODEL	EXPERIMENTAL	MODEL
Temp.	88,5	88,4	84,0	84,1
ζ	0,464	0,444	0,786	0,790
N_3	$-0{,}14\times10^{-5}$	$-0{,}15\times10^{-5}$	$-0{,}57\times10^{-6}$	$-0{,}54\times10^{-6}$
pH	5,0	4,7	4,9	5,03
A_1	3,73	3,03	4,00	4,17
A_2	3,38	3,03	3,99	4,17
A_4	0,03	0,0026	0,059	0,07
C_1	6,50	3,30	5,20	5,38
C_2	2,38	1,30	3,11	3,18
C_3	3,98	2,02	2,06	2,20
Q_d	0,091	0,087	0,269	0,267
Q_a	0,076	0,103	0,249	0,245

	RUN 3		RUN 4	
	EXPERIMENTAL	MODEL	EXPERIMENTAL	MODEL
Temp.	83,0	84,5	87,0	87,8
ζ	1,0	0,989	0,810	0,795
N_3	0,0	$-0{,}3\times10^{-7}$	$-0{,}51\times10^{-6}$	$-0{,}55\times10^{-6}$
pH	4,6	4,8	4,8	4,7
A_1	3,64	3,62	3,88	3,89
A_2	3,56	3,62	3,74	3,89
A_4	0,002	0,0019	0,01	0,0095
C_1	5,28	5,29	5,70	5,62
C_2	2,43	2,63	2,49	2,49
C_3	2,76	2,66	3,10	3,13
Q_d	0,266	0,265	0,187	0,186
Q_a	0,257	0,246	0,167	0,163

	RUN 5		RUN 6	
	EXPERIMENTAL	MODEL	EXPERIMENTAL	MODEL
Temp.	77,0	76,6	75,0	73,9
ζ	1,0	1,0	1,0	1,0
N_3	0,0	$0,1\times10^{-7}$	$-0,14\times10^{-7}$	$0,23\times10^{-8}$
pH	5,0	4,8	5,0	5,2
A_1	4,00	3,95	4,31	4,27
A_2	3,99	3,95	4,25	4,27
A_4	0,0055	0,006	0,013	0,015
C_1	5,00	4,94	4,94	4,95
C_2	3,24	3,29	3,74	3,77
C_3	1,68	1,65	1,12	1,18
Q_d	0,464	0,464	0,590	0,589
Q_a	0,437	0,440	0,569	0,567

	RUN 7		RUN 8	
	EXPERIMENTAL	MODEL	EXPERIMENTAL	MODEL
Temp.	69,0	70,5	81,0	80,3
ζ	1,0	1,0	1,0	0,999
N_3	0,0	$0,71\times10^{-7}$	$-0,26\times10^{-7}$	$-0,3\times10^{-8}$
pH	3,0	4,1	5,0	4,96
A_1	4,48	4,51	4,08	4,18
A_2	4,45	4,51	4,01	4,18
A_4	0,005	0,0046	0,002	0,0021
C_1	5,05	5,01	5,19	5,23
C_2	3,95	3,98	3,34	3,44
C_3	1,05	1,03	1,78	1,79
Q_d	0,759	0,759	0,400	0,398
Q_a	0,732	0,735	0,375	0,374

	RUN 9		RUN 10	
	EXPERIMENTAL	MODEL	EXPERIMENTAL	MODEL
Temp.	60,0	61,5	89,0	90,4
ζ	1,0	1,0	0,955	0,939
N_3	$-0{,}14\times10^{-7}$	$0{,}3\times10^{-7}$	$-0{,}13\times10^{-6}$	$-0{,}18\times10^{-6}$
pH	5,0	5,3	4,9	4,8
A_1	4,30	4,30	4,07	3,97
A_2	4,26	4,30	4,00	3,97
A_4	0,02	0,018	0,03	0,027
C_1	5,27	5,35	5,99	5,93
C_2	3,44	3,50	2,60	2,62
C_3	1,81	1,85	3,30	3,30
Q_d	0,242	0,241	0,233	0,230
Q_o	0,234	0,230	0,216	0,198

	RUN 11		RUN 12	
	EXPERIMENTAL	MODEL	EXPERIMENTAL	MODEL
Temp.	73,0	72,5	83,0	83,9
ζ	0,890	0,910	0,892	0,905
N_3	$-0{,}24\times10^{-6}$	$-0{,}21\times10^{-6}$	$-0{,}31\times10^{-6}$	$-0{,}26\times10^{-6}$
pH	5,1	5,2	4,9	5,1
A_1	4,39	4,34	3,91	4,00
A_2	4,30	4,34	3,87	4,00
A_4	0,03	0,027	0,0089	0,01
C_1	5,24	5,34	5,71	5,77
C_2	3,49	3,53	3,16	3,16
C_3	1,78	1,82	2,53	2,62
Q_d	0,287	0,286	0,276	0,274
Q_o	0,265	0,270	0,252	0,249

7.14 Fortran program of model

```
C       INITIALISING LOOP
        REAL MU,NOUT,NCELL,IPHM,I,K
        READ(5,100)IN,ENA,I,ANA,O,DIFF1,DIFF2,DIFF3
100     FORMAT(G2.0,7F3.0)
        FARDAY=96500
        ZNA=1.
        ZOH=-1.
        P=8.31
        TEMP=75
C       ASSUME CL2 EFFICIENCY=1.
99      AZLTA=1.
C       ASSUME NA EFFICIENCY=1.
C       ASSUME CELL TEMPERATURE
        TEMP1=TEMP
C       CALCULATE CL2 PRODUCTION RATE
        PRDCL2=I*AZLTA/(2*FARDAY)
C       CALCULATE CATH LOST WITH CL2
        ATEMP1=TEMP+273.
        X=37.11-TEMP
        AA=3.46E-3
        BB=5.69E-5
        CC=1.17623E-8
        DD=2.10765E-13
        PRESS1=10**(7.2132-(X/(ATEMP1))*(AA+BB*X+CC*X**2)/(1.+DD*X))
        APRESS=(1.-((PNA*1000.+3.)*(1.9776E-3-1.1756E-5*TEMP)+.035)*PNA*1000
        *)*PRESS1
        ALOSS=PRDCL2*APRESS/(630-ANOLESS)
        AMASS=ALOSS*(1.+PRDCL2*2.)
C       CALCULATE H2 PRODUCTION RATE
        PRDH2=(I/(2*FARDAY)
        CLOSS=ALOSS
        CMASS=CLOSS*(1.+PRDH2*2.)
C       CALCULATE MASS FLOW RATES AT DIAPHRAM AND OUTLET
        MOUTRT=CMASS+CMASS
        MDIPHRM=IN-ANARTS
C       CALCULATE THICKNESS
        PNA=TEMP*(1.7547E-3+2.3E-5*(1.+PNA*1000.*3.)
        A=1.0006679E-1.1637E-3*ATEMP+5.1792E-5*TEMP**2+1.2540320E-8*TEMP
        **3
        B=(7.4662850E-03-2.3408720E-5*TEMP+3.0564220E-7*TEMP**2-9.3403150E-
        10*TEMP**3)*PNA*T
        C=(1.9376E-2-2.2301480E-7*TEMP-5.1481250E-9*TEMP**2+1.7915370E-
        11*TEMP**3)*PNA*T**2
        AGNDTY=A+B+C
C       CALCULATE FLUID RATES
        VDIPHM=MDIPHM/AGNDTY
        CDUT=MOUT/AGNDTY
        VDIPHM=VDIPHM/AREA
C       CALCULATE COMPONENT BALANCES
        VIN=IN/AGNDTY
        CNA=IN*ENA/COUT
        CCL=(1.-ENA-2*PRDCL2)/COUT
        CDH=CCL
C       CALCULATE ION TRANSFERENCE NUMBER
        CNACL=(((CNA+CDH)/2)*(1.-2.))/(AGNDTY-((CNA+CL)/2)*58.453)
        TNACL=(1.-(1.-.3667*T-.0012*T**2)*(-1.2719E-3+3.9405E-6*TEMP)*CNACL+(.
        *1100-3.998E-5*ATEMP)*CNACL**2+(-1.2971E-3+3.9405E-6*TEMP)*CNACL
        **3)
C       CALCULATE ANOLYTE CONCENTRATIONS
        FLUXNA=IN*ENA/AREA
        FLUXCL=(IN*ENA-I/FARDAY)/AREA
        ESS=(FLUXNA-TNACL*I/(FARDAY*AREA)-CNA*(TNACL*DIFF1/D-DIFF1/D)+TNACL
        *DIFF2*CCL/2)*TNACL*DIFF3*CDH/D-VDIPHM*CNA/2)
        FFF=(VDIPHM/2*TNACL*DIFF2/D-TNACL*DIFF1/D*(-DIFF1/D)
        ANA=FFF/FF
        ACL=ANA
C       CALCULATE ION MIGRATION RATE
        TIME=CDUT*VDIPHM/(FLUXCL*AREA)
        FLUXCL=TIME*(ACL*FARDAY*AREA)-DIFF3*CDH/D*VDIPHM*CDH/2
C       CALCULATE EFFICIENCY
        AZLTA=1.+FLUXCL*AREA*FARDAY/I
```

```
      ACL1=ACL
      CCL1=CCL
      COH1=COH
      IF(AZETA-1)101,101,102
102   AZETA=1
101   AZETA1=AZETA
C     CALCULATE CELL TEMPERATURE
      V=1*1.0706*+50
      U=V*1**.5
      HREACT=PHDCL2*46896.9
      TEMPF=1.344*MIN+23.7
      TCHMI=5.567*+**450*PNDCL2*(70.9*.1105+2*3.475)+MOUT*.83+(ALOSS+CL)3
     *5)*16*.45
      TERM2=GAMINV.83*(TEMPF-25)*PNDCL2*(70.9*.1105*25+2*3.475*25)+MOUT*
     *.83*25-(ALOSS+CLOSS)*(1*71+1.961*.5*16*.15*9.)-HREACT*9.078
      TEMP1=TEMP2/TEMP1
C     IF(ABS(TEMP1-TEMP).GT.0.0)GOTO 99
      WRITE(6,106)
      WRITE(6,105)
104   FORMAT(T33,'RUN NO.  ',I5,14('*'),/)
105   FORMAT(T33,'RESULTS OF INITIALIZING LOOP')
      WRITE(6,207)
      WRITE(6,208)
      WRITE(6,209)'MOUT','COUT','MOIPHM','MOIPHM','CNA','CCL','COH','APRESS'
202   FORMAT(/,T2,'MOUT',T21,'COUT',T37,'MOIPHM',T51,'MOIPHM',T65,'CNA'
     *,T77,'CCL',T92,'COH',T104,'APRESS')
203   FORMAT(T2,115('*'))
204   FORMAT(T2,3F14.5,//)
      WRITE(6,202)
      WRITE(6,204)
      WRITE(6,207)'AFACL,FLUXH,AZETA,ADMSTY,VDIPAV,TNAGY,TEVP
205   FORMAT(T2,'AFACL',T23,'FLUXH',T47,'AZETA',T65,'ADMSTY',77
     *9,'VDIPAV',T113,'TNAGY',T136,'TEMP')
206   FORMAT(T2,115('*'))
207   FORMAT(T2,5F14.5,//)
      N=0
C     MAIN LOOP
C     CALCULATE ACL2 PRODUCTION RATE
108   AZETA1=AZETA
      PRODCL2=(AZETA/(2+AZETA))
C     CALCULATE ACL2 DEPOSITION RATE
      PRODCL2=(1-AZETA)*(V/(4*DMAY))
C     CALCULATE MASS LOSS OF ACLYTE
      ATOMS=1.4E+23
      X497=.11*TOMS
      AA=3.6497E
      BB=5.9E5*E-3
      CC=1.1723E-5
      DD=2.1E7*E-4
      PHOSS=10.**(-(1.2)2E-(X/(ATOMP))*(AA+BB*X+CC*X**3)/(1.+DD*X))
      APRESS=((1.-((ACL*1000.-3.)*(1.77E-3-1.13E-5*TEMP)+.035)*ACL*1000.
     *)*PHOSS
      ALOSS=(PRODCL2*(PRODCL2*APRESS/(6.3E-4*PRESS)
      CMASS=ALOSS*(1.+EF/(CL**2.+EF))*PRODCL2
C     CALCULATE MASS OF CHLORINATE
      PROMIS=(41./(PRODCL2*Y)
C     CALCULATE MASS OF CATHOLYTE
      IF((CCL**2).LT.1.E-6)GO TO 350
      CPRLOS=((1.-5.E-5*CCL*1000.)-((174.+TEMP)*(-8.)7E-05+3.37E-04*COH-1.33
     *E-6)*COH**2+7.8E-6/COH))*3.C417)*COH*1000)*APRESS
      GO TO 351
350   CPRLOS=((1.-((CCL*1000.-1)*(1.927E-3-1.193E-6*TEMP)+C.C35)*CCL*1000.-(
     *(17.+TEMP)*(-8.)7E-05+3.37E-04*COH-1.33E+1*COH**2+7.88E-6/COH))*C.031
     *7)*CCL*1000.)*PRESS
351   CLOSS=PRODCL2*CPRLOS/(6.3E-4*PRESS)
      CMASS=PRODCL2*(1.+CLOSS)*14
C     CALCULATE MASS FLOW RATES AT DEAERATOR AND OUTLET
      MOUT=V*1.E+3*ATOMS/CMASS
      MOIPHM=MIN*AMASS
C     CALCULATE MOLARITIES
      FNA=1.-FNA*EXP(-.5*CL*E1/(1.+FNA*3.4*E-3))
      ACL=TACL*1000.*(1.-4.4E-3*(1.+ACL*34.+53.))
      CCL=TCCL*1000.*(1.-4.4E-3*(1.+CCL*34.+53.))
      COH=TCOH*1000.*C/(1.+COH*40.)
      AAA=1.3C467-7.1E-3*(.4774+)-0.*E-MPF*5.17920730-6*TEMPF**2+1.0E4*32D-4*
     *TEMPF**3
      BBB=(7.45C-3*0.-23-2.6E5*730-6*TEMPF+3.0E4*2350-7*TEMPF**2-9.34033
     *1E0-10*TEMPF**3)
```

```
      CCC=(1.+.637*(C5D-05*4.23D-1850-7*TEMPF-5.14*3.1250-9*TEMPF**2+1.79*3
     #7D-11*TEMPF**3)
      FDNSTY=SNGL(A+B*PHWT+CCC*PHWT**2
      A=1.+CC*(-7.1647*9)-6*TEMP-5.17920750-5*TEMP**2+1.0540320-9*TEMP
     **3
      B=(7.+5.2E-50-03-2.+5.3720-5*TEMP+3.05*3.2D0-7*TEMP**2-9.340331D0-
     #10*TEMP**3)*ACLWT
      C=(1.+.6*(-.7544.D3D1.35D-7*TEMP-5.14*3.125D-9*TEMP**2+1.794537D-
     *11*TEMP**3)*ACLWT**2
      ADNSTY=DNSTY
      DUD=1.3668*1.1475E7D-02*COHWT-1.722D3D-5*COHWT**2-3.565138D-4*TE
     *MP
      CCC=-2.143812D-06*TEMP**2+7.65D02D-1*CCLWT
      CDNSTY=DUD*CCC
C     CALCULATE VELOCITY FACTOR
      VOIPHM=VOIPHM/ADNSTY
      VOUT=VOUT/CDNSTY
      VOIPHM=VOIPHM/AREA
C     CALCULATE CELL MOMENT BALANCES
      QTIRET=QPERSTY
      CNA=CINMENA/QOUT
      CCL=(CINMECL-2*PROCL2)/QOUT
      COH=CNA-CCL
C     CALCULATE DATA ANGLE DEVIATION
      CNACL=(ACL*1000)/(ATAN(TY=ACL*0.05))
      TNAGY=.4*(-1.*(CNA)+.8*TEMP*(-.0311*CNA+1.+.852E-4*TEMP)*CNACL*(.3
     *1158-3.36E-5*TEMP+3.E-7*TEMP**2)*CNACL**2+(-1.27194-3+3.04*E-6*TEMP)*CNACL
     **3
C     CALCULATE ANGULYTIC CONCENTRATIONS
      FLUXNA=DIN/AREA
      FLUXCL=(DIN-PROCL2)/AREA
      CE=(FLUXNA-1.*TNAGY/(1.DAY*AREA)-CNA*(TNAGY*DIFF1/D-DIFF1/D)+TNAGY
     *DIFF2*CCL/2*TNAGY*DIFF3*(CNA/2-VOIPHM*CNA/2)
      FF=(VOIPHM/2*TNAGY*DIFF2/2-TNAGY*DIFF1/D*DIFF1/D)
      ANA=CE/FF
      ACL=ANA
C     CALCULATE MEMBRANE MIGRATION RATE
      IF(ACL.GT.0.)GO TO 303
      FLUXCHET=(1/(2*FARADAY*ANCA)-DIFF3*COH/D+VOIPHM*CNA/2
C     CALCULATE EFFICIENCY
      ACETA=1.+FLUXCHET*2*FARADAY/I
      IF(ACETA-1)302,302,303
303   ACETA=1
302   N=1
C     CALCULATE PH OF ANOLYTE
      FOR=(1-ACETA)*3/AREA
      IF(I62)1,2,1
2     I62=I62+3
1     AA=6.3115E-04+1.4409E-0*TEMP-1.913E5E-1*ACL
      YY=(1/AREA)*3.63
      PH=(ALOG(10)*ALOG(XX)-ALOG(YY))/1.15129
      DELPH=-1.5*2.*ACL
      APH=PH+DELPH
C     CALCULATING CONCENTRATION OF MINOR COMPONENTS
      AVCL=ABS(ACL)
      AHCL=EXP(-1.*.5*E-.3.8D*10E-3*TEMP+5.9213E-2*ACL+1.000+2.3259*PH)
      AOCL=(AHCL)*(2.*E-7*EXP(-1.*5.6/(ATMP+2)))/(10**(-PH))
      PROCL2=2.*5.*AREA*(.5*.5E0*TEMP)*AHCL**2*VOCL*AVCL
      AHCL=AHCL*1.E-3
      AOCL=AOCL*1.E-3
      WRITE(6,6C0)
600   FORMAT(T5,'RESULTS OF MAIN LOOP')
      WRITE(6,601)
401   FORMAT(T5,'LOOP NO.',T15,I3)
      WRITE(6,602)
      WRITE(6,403)
      WRITE(6,404)CDUT,VOUT,VOIPHM,VOIPNA,VOIPCL,CNA,CCL,COH
402   FORMAT(/,T5,'VOUT',T23,'VOUT',T37,'VOIPHM',T51,'VOIPNA',T65,'VOI
     #CL',/,T5,'CNA',T23,'CCL',T37,'COH')
403   FORMAT(T2,13A('*'))
404   FORMAT(T2,'T=',5.2//)
      WRITE(6,405)
      WRITE(6,406)
      WRITE(6,407)ANA,ACL,FLUXDH,ACETA,PH,APH
405   FORMAT(T5,'ANA',T23,'ACL',T37,'FLUXDH',T51,'ACETA',T65,'PH',T79,'A
     #PH')
406   FORMAT(T2,80('*'))
407   FORMAT(T2,6(E14.5,2X))
```

```
      WRITE(6,501)
      WRITE(6,503)
      WRITE(6,502)AHOCL,ACCL,PRCL33
  501 FORMAT(1X,'AHOCL',T23,'ACCL',T37,'PRCL33')
  502 FORMAT(F6.4,F6.4)
  503 FORMAT(T2,'ZETA',5X//)
      IF(ALOG(AZETA-AZETA(I)-.002)*00.900.100
  900 STOP
      END
```

Author Cook Peter Gavin
Name of thesis A Mathematical Model Of A Diaphragm-type Chlor-alkali Cell. 1978

PUBLISHER:
University of the Witwatersrand, Johannesburg
©2013

LEGAL NOTICES:

Copyright Notice: All materials on the University of the Witwatersrand, Johannesburg Library website are protected by South African copyright law and may not be distributed, transmitted, displayed, or otherwise published in any format, without the prior written permission of the copyright owner.

Disclaimer and Terms of Use: Provided that you maintain all copyright and other notices contained therein, you may download material (one machine readable copy and one print copy per page) for your personal and/or educational non-commercial use only.

The University of the Witwatersrand, Johannesburg, is not responsible for any errors or omissions and excludes any and all liability for any errors in or omissions from the information on the Library website.